Hydrogeological model of Los Humeros: hydrothermal processes at the regional scale

D 3.3

Hydrogeological model of Los Humeros: hydrothermal processes at the regional scale

Version 1

Armandine Les Landes Antoine; Maurel Camille; Lopez Simon; Calcagno Philippe

Work package 3

Due to 03-13-2019

Website: http://www.gemex-h2020.eu

The GEMex project is supported by the European Union's Horizon 2020 programme for Research and Innovation under grant agreement No 727550

Table of Contents[1]

[1] The content of this report reflects only the authors' view. The Innovation and Networks Executive Agency (INEA) is not responsible for any use that may be made of the information it contains.

List of figures

List of tables

Executive summary

This report is prepared by the BRGM (*Bureau de Recherches géologiques et Minières*) of France as deliverable 3.3 of work package 3 for GEMex (Grant Agreement No. 727550).

The report describes the regional hydrogeological model of Los Humeros. Numerical simulations were carried out to model the geothermal system through the resolution of mass flow and heat transport equations in a fractured porous media. The simulation code used in this study is ComPASS

Introduction

The aim of GEMex project is to obtain a better understanding of the geothermal field, especially of the location of these super-hot fluids and the way to exploit them. Conceptual and simulation models have been developed over time at local scale, inside the main structures, to characterize the reservoir behaviour and determine the hydrothermal conditions at natural state (Arellano et al., 2003, 2015). The task 3.2 of GEMex project, presented in this report, intends to propose an hydrogeological and thermal model of Los Humeros at regional scale and contribute to the general understanding of heat sources nature, their location, and influence on flow dynamic at a boarder setting than the geothermal field and the major structure of Los Humeros (LH) and Los Potreros (LP).

Los Humeros is a geothermal field within a Quaternary volcanic complex with an existing geothermal power plant in operation since 1990. Our research focused on an improved and comprehensive understanding of the location and characteristics of the deeper superhot/supercritical geothermal reservoir and its connection to the known conventional geothermal system.

This document is organized as follow:

Section 1 presents the general geological and hydrothermal context of Los Humeros at local and regional scale.

Section 2 presents the hydrothermal model and the methodology used to generate this dynamic model

Section 3 presents the numerical solution used for simulations, the mesh generation, boundary conditions and properties implemented.

Section 4 presents the general results and conclusion from the hydrothermal modelling of the geothermal field and its region.

Section 5 introduces the development perspectives and improvements that are currently being considered for future simulation over Los Humeros regional field.

1 Geological and hydrothermal context of Los Humeros

1.1 General settings

Los Humeros volcanic complex (LHVC) is located about 270 km East of Mexico City and 200 km West of the Atlantic coast along the Trans Mexican Volcanic Belt (TMVB) ; a major structure that runs across central Mexico, from coast to coast, over 900 km long and 130 km large (Figure 1). Volcanic activity is reported to have started about 16 Ma ago (Ferrari et al., 1999) and continues today with several active volcanoes. The LHVC is structured by Los Potreros caldera interlocked inside a larger caldera: Los Humeros. The system is part of a set of siliceous volcanic complexes of the Pleistocene its last eruption taking place 0.46 Mya.

Four geothermal fields are currently operating along the TMVB and Los Humeros is the third largest field to be currently in operation. The exploration started in 1968 in the area and the first well was drilled in 1981. Commercial operations begun in 1990 with an installation of 5 MWe and todays installed capacity reaches 94 MW. The electricity is generated from around 25 wells producing 6 million tons of steam per year (IEA Geothermal, 2018). The geothermal field is operated by the *Comisión Federal de Electricidad* (CFE).

Figure 1: Location of Los Humeros thermal field along the TMVB (Jentsch and Jolie, 2017)

The maximum temperature measured at approximately 2.5 km depth reaches around 400 C, but no geothermal fluid is being exploited by CFE at this depth for the time being (Calcagno et al., 2018). Los Humeros is currently a conventional hydrothermal system, with locally super-hot untapped fluids at high depth.

1.2 Geological context

The LHVC has been studied and exploited for decades (Carrasco-Núñez et al., 2017; López-Hernández, 1995). Carrasco-Núñez et al., (2018, 2017) have recently produced a revised geological map of the Los Humeros area and a reappraisal of its geologic evolution (Figure 2).

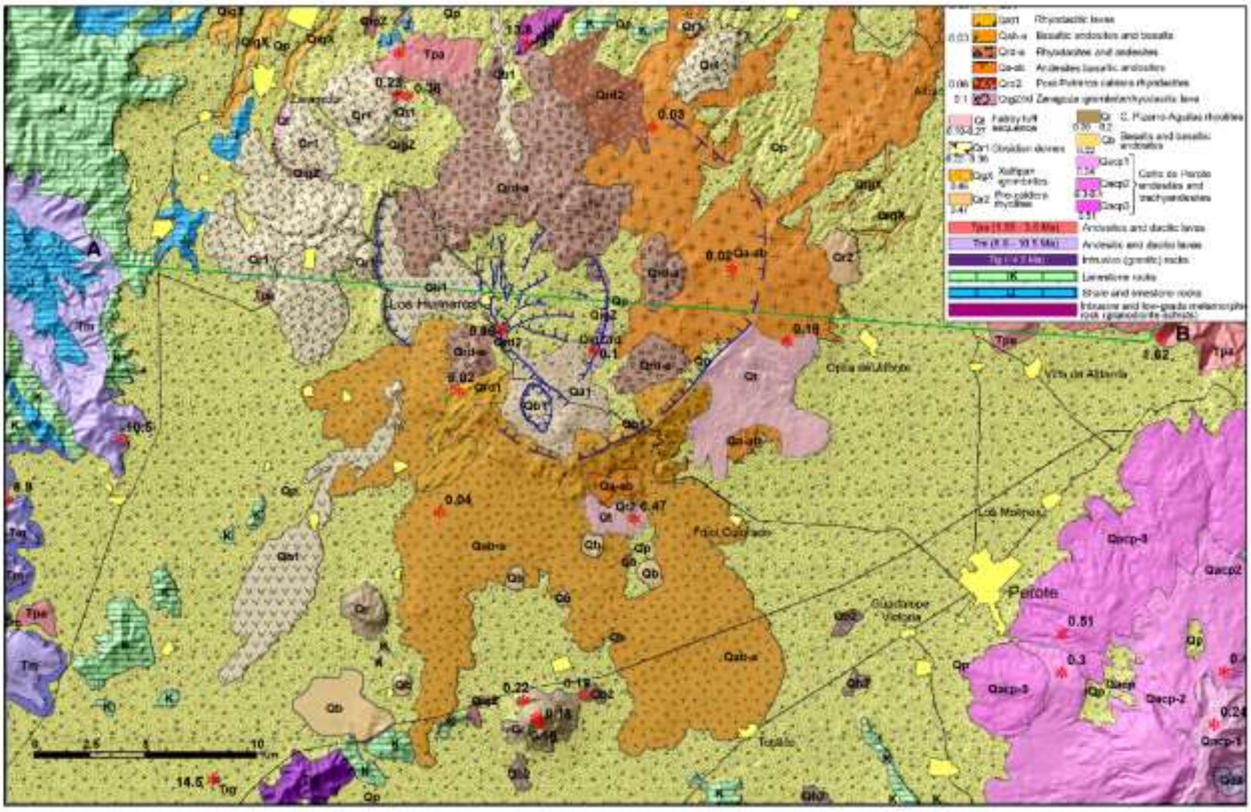

Figure 2: Geological map of Los Humeros adapted from Carrasco-Núñez et al. (2017b)

1.2.1 Geological formation

Geomorphologically, the LHVC is an 18 to 20 km-wide circular caldera structure, with an inner and younger subordinate 5–8 km-wide oval caldera (Los Potreros) (Calcagno et al., 2018). Geologically, it is a Pleistocene basalt-andesite-rhyolite system with geothermal activity currently being exploited. It is the northernmost volcano of the Serdán-Oriental Basin (SOB), which lies West of the andesitic stratovolcanoes forming the Citlaltépetl-Cofre de Perote volcanic range.

The Los Humeros volcanic complex is characterized by a multistage formation, with at least two major episodes of caldera collapse: the Los Humeros caldera and the Los Potreros caldera formed at 460 and 100 kya, respectively (Ferriz and Mahood, 1984). However, recent work based on modern geochronological dating methods (U/Th and precise $^{40}Ar/^{39}Ar$) has revealed a much younger formation age of these calderas at 165 (Los Humeros) and 70 kya (Los Potreros) (Carrasco-Núñez et al., 2018).

From a geothermal standpoint, the geological formations of the Los Humeros area consist of four groups. In addition to the **basement** (first group), it is important to separate the volcanic formations into three distinct groups: **Pre-caldera, Caldera, and Post-Caldera** (Table 1). For a more detailed interpretation of the geothermal system, these four can be split into nine units as presented by Calcagno et al., (2018): Basement,

basal Pre-Caldera, intermediate Pre-Caldera, upper Pre-Caldera, Los Humeros Caldera, intermediate Caldera, Los Potreros Caldera, Post-Caldera, and undefined pyroclastic deposits.

Table 1: Description of the geological formations modelled in Los Humeros at regional scale gathered into four groups and nine units (Calcagno et al., 2018)

Group	Unit	Rock	Age (Ma)
G1 Post-caldera	U1 Undefined pyroclastic	Tuff, pumice and some alluvium	< 0.003
	U2 Post-caldera	Rhyodacite, andesite, basaltic andesite, and olivine basalt lava flows	0.050 to 0.003
G2 Caldera	U3 Los Potreros caldera	Rhyodacitic flows	
		Zaragoza ignimbrite	0.069
	U4 Intermediate caldera	Faby tuff with andesitic-dacitic lava flows	0.07
		Rhyolitic and obsidian domes	0.074
	U5 Los Humeros caldera	Mainly composed of Xaltipan ignimbrite with minor andesitic and rhyolitic lava	0.165
G3 Pre-caldera	U6 Upper pre-caldera	Rhyolite, dacite, some andesite and tuff, and minor basalt	0.693 to 0.155
	U7 Intermediate pre-caldera	Mainly pyroxene andesite (Teziutlán andesite) with mafic andesite in the basal part and/or dacite	2.61 to 1.46
	U8 Basal pre-caldera	Mainly hornblende andesite (Alseseca andesite and Cerro Grande) and subordinate dacite	10.5 to 8.9
G4 Basement	U9 Basement	Middle Miocene granite	15.12
		Cretacic limestone, shale and minor flint	~140
		Jurassic limestone and shale	~190
		Paleozoic granite and schist (Teziutlán Massif)	>251

According to this geological synthesis, main hydrogeological characteristics have been described. From to the top to the bottom, the first unit (Post-caldera) contains shallow aquifers, some of them locally thermal. This unit forms shallow and cold aquifers and is characterized by high-medium permeability. The second unit (Caldera) forms an aquitard and acts as a seal-cap (low permeability). The third one (Pre-caldera) contains the geothermal fluids (medium-low permeability) and the fourth (Basement) is characterized by low permeability and high temperature (Gutiérrez-Negrín et al., 2010). Then, **the geothermal target is mostly located in the Pre-Caldera volcanic rocks** (mainly andesite), but it is also expected to find superhot fluids in portions of the underlying carbonate-rock basement that may present secondary permeability.

1.2.2 Fault system

Regional faults, present outside the principal and largest rim of Los Humeros caldera, are inferred structures and were described by López-Hernández, 1995.

The basement of LHVC has been deformed by two main tectonic events (Late Cretaceous to Paleocene contraction and Eocene-Pilocene extension) that produced N-S to N-E striking faults (Campos-Enriquez and Garduño-Monroy, 1987; López-Hernández, 1995). The rims of Los Humeros and Los Potreros have been interpreted as landslide generated by the calderas collapse along outward dipping ring faults (Norini et al., 2015). The deformation is defined by the coexistence of two volcanic strucutral systems: a circular collapse caldera faults and morphological rims of Los Humeros and Los Potreros Calderas and another system represented by NNW-SSE, N-S, NE-SW and E-W striking fault on the floor of Los Potreros Caldera. According to Norini et al., (2015), the first collapse recalls an asymetric trap-door strucutre and impinges on a thick volcanic succession (10.1 to 1.55 Mya), now hosting the geothermal reservoir.

The producing geothermal wells in the Los Humeros geothermal field (LHGF) are placed along the main NNW–SSE active faults in the eastern part of LP caldera (Figure 3) or near pervasive N-S striking faults splays in the central-northern sector of LP caldera (Norini et al., 2015).

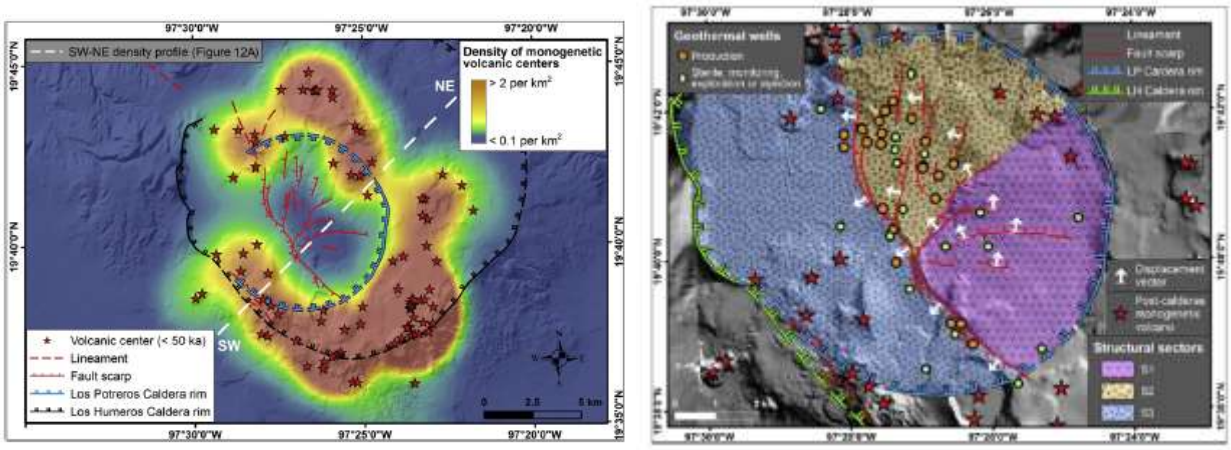

Figure 3: Density map of LHVC post-calderas monogenetic volcanic centers (left) and morpho-structural interpretation of the three main structure sectors identified in the LP and LH calderas (right) from (Norini et al., 2015)

The distribution of faults and lithostratigraphic units along an E-W structural cross section over LHVC are shown in Figure 4. The nine different lithostratigraphic units belong to 4 main groups: regional meta-sedimentary basement and 3 volcanic groups (Pre-Caldera, Caldera and Post-Caldera) (cf. Table 1). The structures that dominate the geothermal field of Los Humeros Caldera are really important (hydraulically speaking), as they are expected to act as "conduits" for heat transfer.

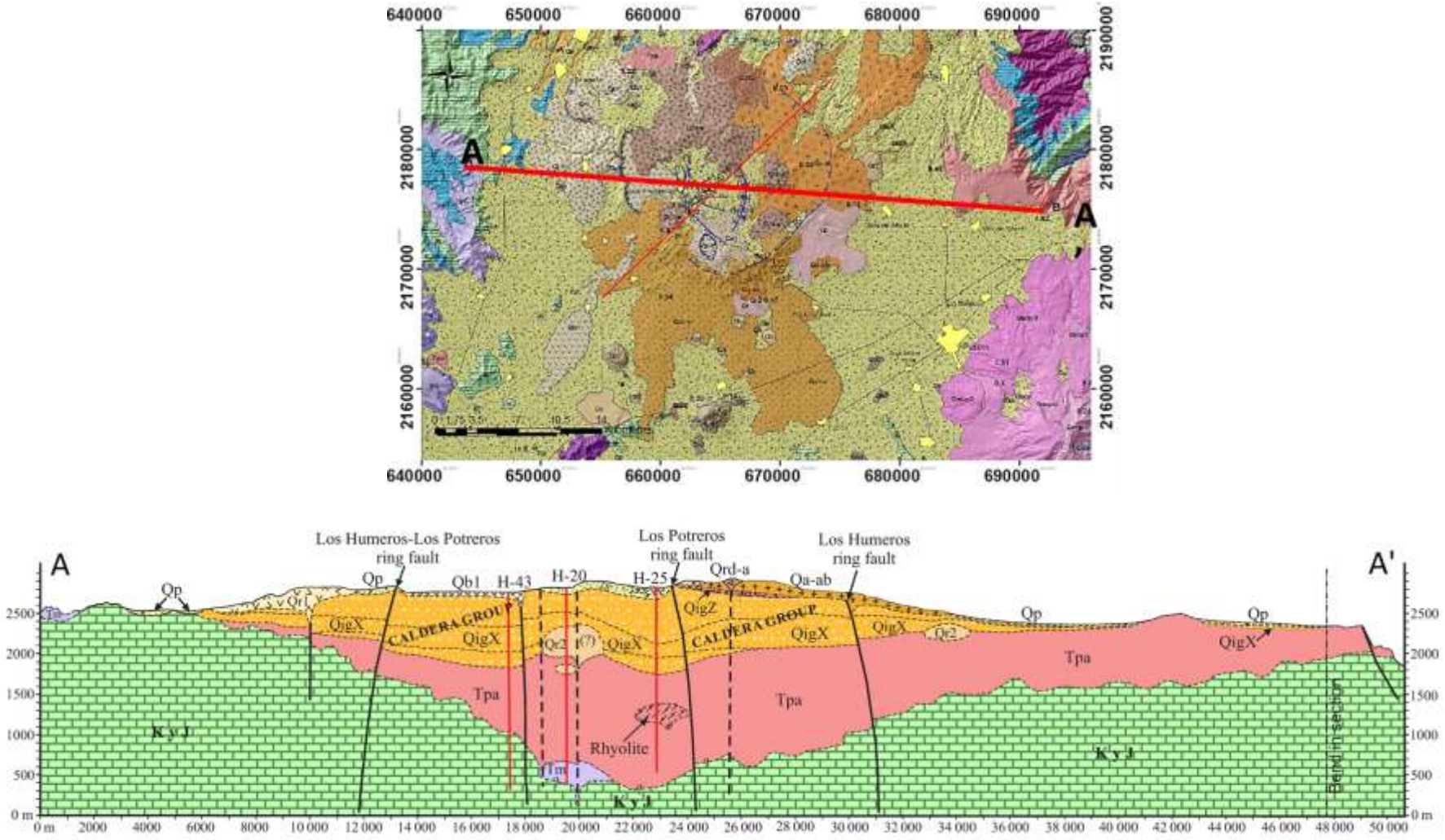

Figure 4: Top: Geological map and Bottom: Cross section form West (left) to East (right) of the Los Humeros caldera (Carrasco-Núñez et al., 2017). K y J (Green) is the limestone basement, considered as a low permeability layer. Tpa (pink) is the Pre-Caldera group where lie the two identified reservoirs (Cedillo Rodríguez, 2000). This layer outcrops in the Eastern part where the regional recharge is thought to occur.

1.3 Hydrogeological context

1.3.1 General context

Los Humeros reservoir has been extensively studied by Jimenez-Salgado, (2014) at regional scale. Los Humeros is a liquid dominated field where the permeability is mainly related to the presence of faults and to the structural deformation occurring in this area.

1.3.2 Recharge

Three watersheds are influencing the geothermal system of Los Humeros (Figure 5):

- Los Humeros;
- Tepeyhualco;
- Perote.

The regional recharges is suggested to come from precipitation in the area and especially from the Eastern part where a large part of the reservoir layer outcrops.

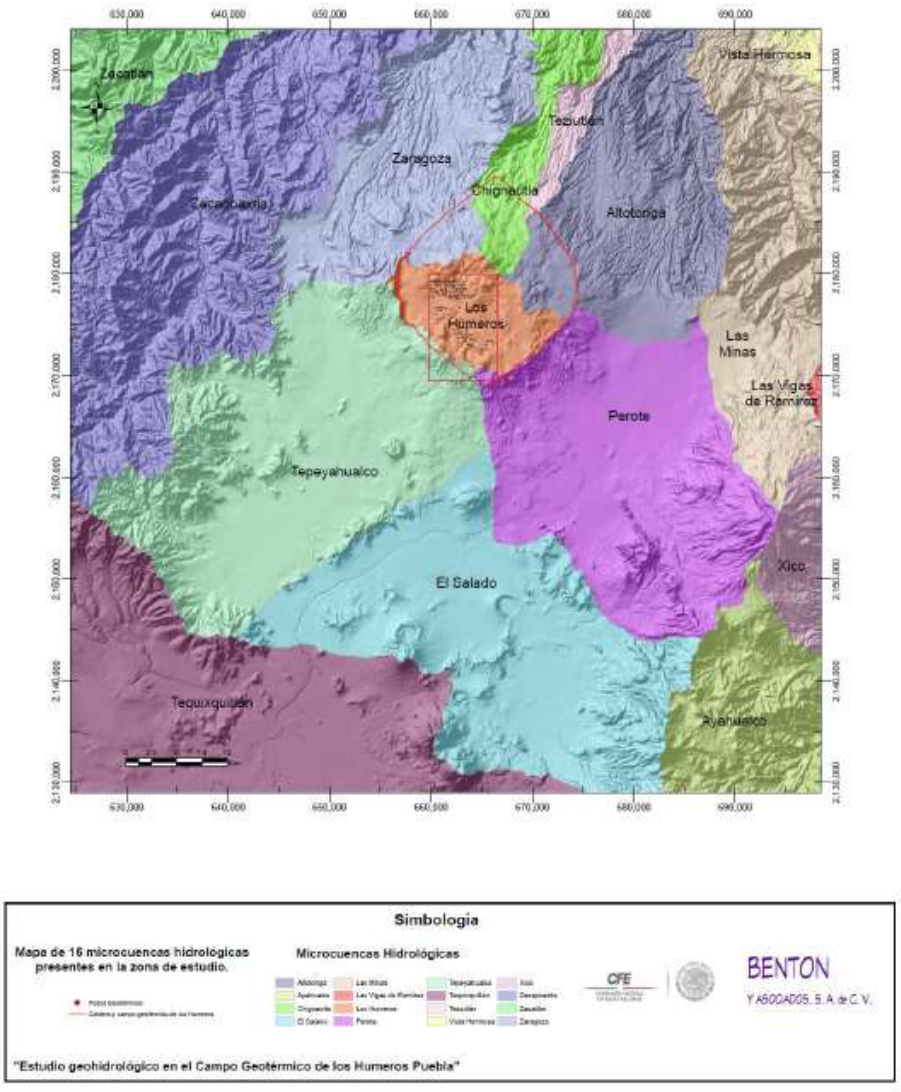

Figure 5: Map of watersheds around LHVC (Jimenez-Salgado, 2014)

The map of water head (Figure 6) suggests that water is drained from Tepeyhualco and Perote watersheds toward the south part of Los Humeros Caldera. The point of intersection between the three watersheds is thus suggested to be the principal convergence point.

Table 2: Hydro meteorological balance (Jimenez-Salgado, 2014)

Name	Infiltration (I) in Mm3	Extraction (E) in Mm3/y	Exceeding volume in Mm3/y
Los Humeros	55.22	0.79	51.43
Perote	260.47	10.07	250.4
Tepeyhualco	92.00	3.22	88.78
TOTAL			390.61

Infiltration inside the caldera (Table 2) is important as suggested by the hydro-meteorological balance calculated by Jimenez-Salgado, (2014). Total recharge is estimate to 390 Mm3/year for the shallow aquifers acting on the LHVC. However, infiltration of this meteorological recharge in the deep geothermal system has not been estimated.

According to Cedillo Rodríguez, (2000, 1999) studies based on investigations along wells of 200 to 400 m depth situated inside and outside of the Caldera of Los Humeros have shown two ground water systems. One warmer than the other and both being delimited by fault systems, the ground water is found in basalts, tuffs and andesites. Cedillo Rodríguez, (2000) suggests that the discharge is mainly carried out through faults and fractures to deeper levels where geothermal reservoirs are located.

The topography is also influencing the recharge through rainfall. Indeed, high points are located along LH and LP caldera rims and in the area of El Cofre de Perote, South-East of the caldera (Figure 6).

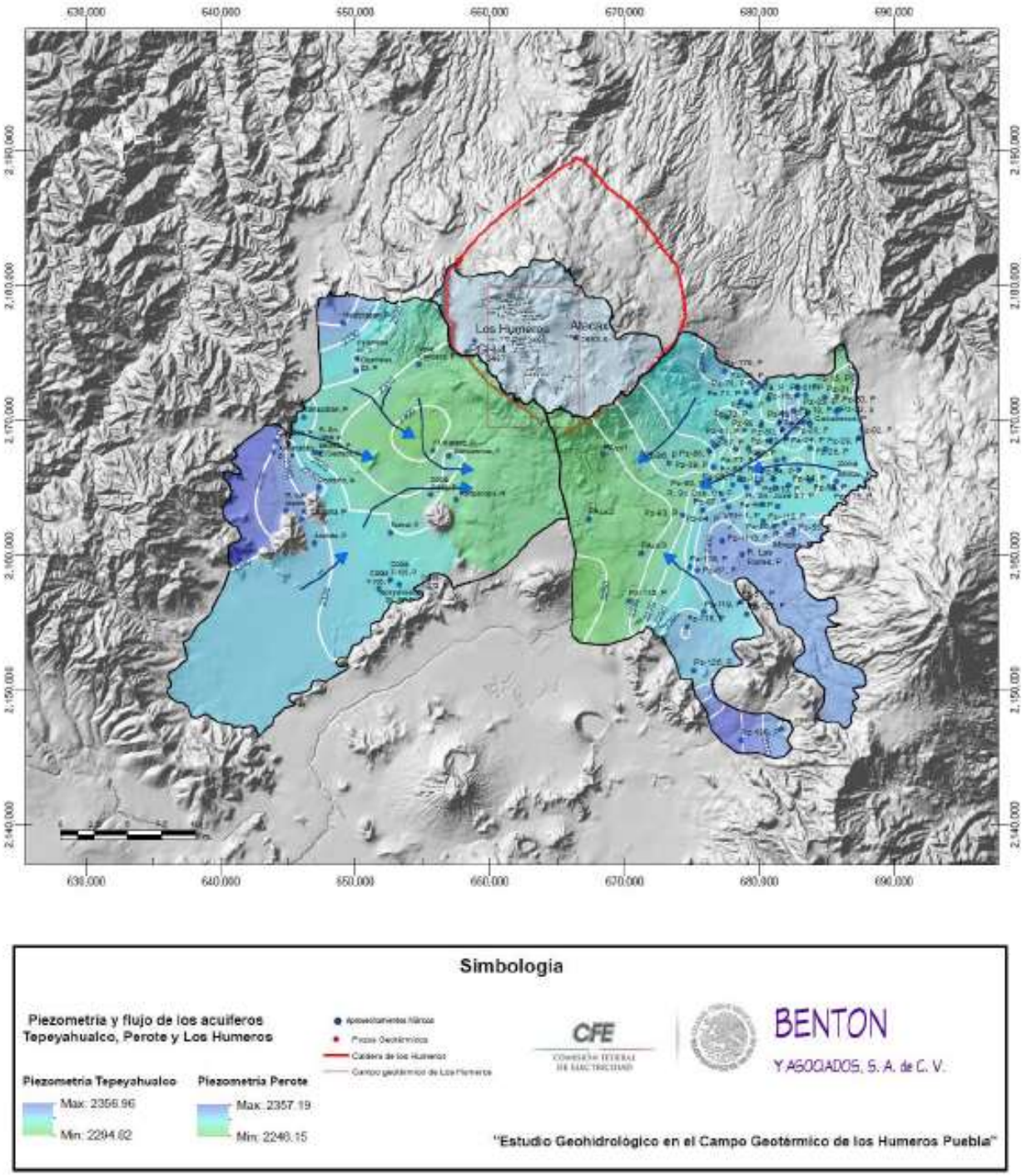

Figure 6: Water head map in Los Humeros, Tepeyhualco and Perote watersheds (Jimenez-Salgado, 2014)

1.4 Geochemical context

Field work and laboratory analysis have been conducted in Los Humeros geothermal field as part of WP4 of the GEMex project. The principal objectives of the study of fluid geochemistry concerned the identification of the main recharge, the physico-chemical evolution of hot fluids and the identification of flow paths in the fractured porous media of LHGF.

Sampling of water and gas from natural manifestations, water wells and geothermal wells have been collected before being analysed in laboratory along with in-situ measurements. The work was performed at regional scale which constitute the main improvement when comparing to previous work on LHVS.

The results of the investigation have shown that stable isotope compositions of geothermal fluids are compatible with processes commonly found in geothermal wells which suggests that there is a strong interaction of meteoric water with reservoir rocks. The understanding of the role of meteoritic component and its characterization at regional level have been improved through GEMex studies.

Geothermomerters analysis suggested temperature values of 320 +/- 30°C for the deep diluted geothermal waters. Water collected from Los Humeros wells are mainly constituted of shallow water rich in Ca, Mg and are enriched in Boron suggesting small inflow of high-temperature deep water (close to 300°C) despite low permeability in deep formation (Caldera, Pre-Caldera and below).

The analysis of degassing soil in LHGF showed that there is a good correlation between known faults and the increasing in CO_2 flux, elevated Radon and Thoron concentrations. Along with other analysis of carbon isotope of CO_2, gas study suggests the presence of convection along permeable faults and the existence of links between deep geothermal reservoirs and subsurface fractures and faults. The up-flow of hydrothermal fluids is favoured with faults. The most permeable zone when considering soil degassing is located in SW area and extends towards the N and NE.

Fluid-rock interaction in LH have also been studied through GEMex project at various temperatures and pressures. The main results indicate that silicification is the most important alteration in the geothermal system and that infiltrated water may react with intersected formation before reaching the reservoir.

1.5 Geothermal structure of Los Humeros

1.5.1 Thermal structure

According to Norini et al., (2015), the surface thermal anomalies show some geometric relation with the main structures - western boundary of the resurgent area along the main NNW-SSE active faults and minor fault splays inside Los Potreros caldera - as shown in Figure 7. Their study also suggests that geothermal fluids are driven directly to shallow level along the sub-vertical faults. As the reservoir is sealed by thick LHVC post-calderas volcanism units, the heat source is probably located deeper below the LP and LH sector and is associated with magmatic intrusions and geothermal fluid circulation or diffuse heat source.

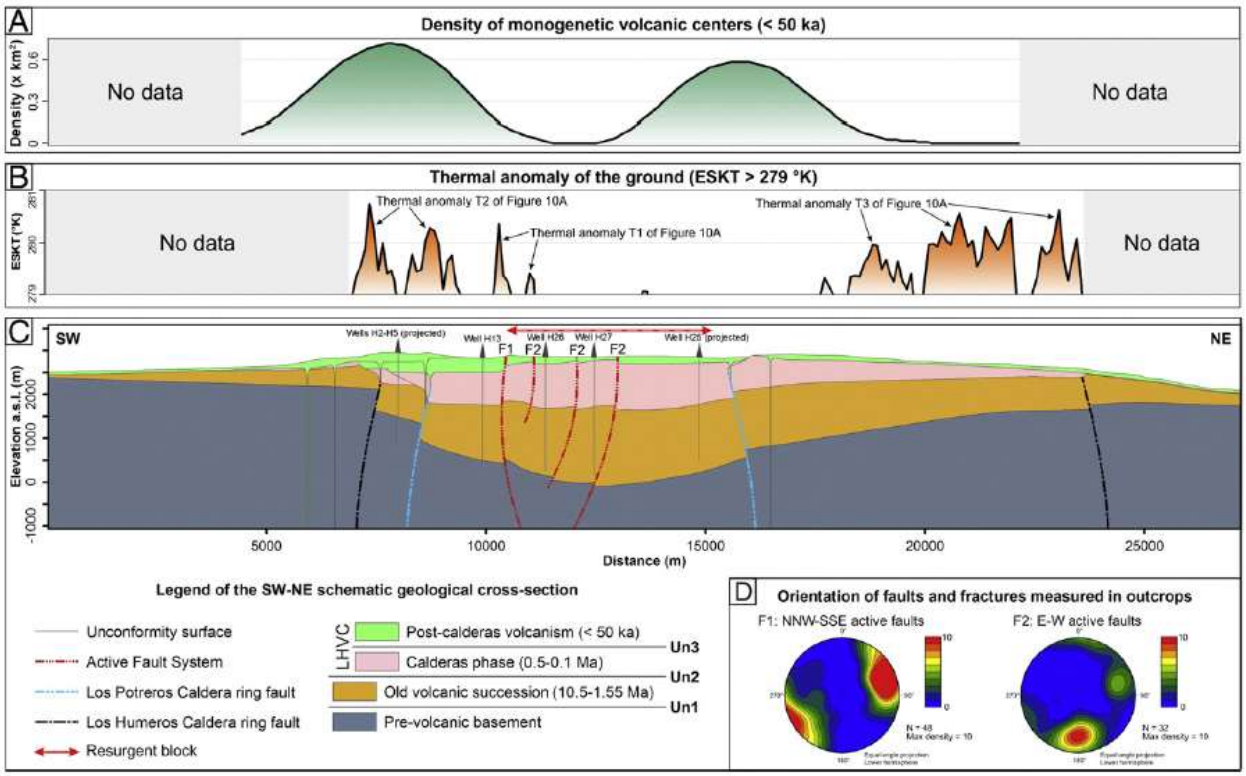

Figure 7: Density profile (A), thermal anomaly of the ground from enhanced SKT profile (B) Enhanced SKT profile (°K) along the SW–NE trace and (C) schematic geological cross-section of LHVC SW-SE trace and (D) density plot of faults and fractures collected in the field from (Norini et al., 2015).

The origin of heat source could not be identified by wells because of their depth. Limberger et al., (2018) while studying the thermal structure of Los Humeros proposed different depth and position estimation of the magmatic chamber when considering either parts or all available temperature measurement from CFE. In the first case, the magmatic chamber location was positioned at 4100 meter above sea level (m a.s.l.) to allow a reasonable fit of the wells selected. In the second model, the magmatic chamber emplacement is shallower (around 2300 meters above sea level) but well data are poorly matched suggesting a more complex heat transfer in the thermal field of Los Humeros. Advection from regional flow and convection cells through faults are mentioned as possible forms of heat transfer. The thermal model proposed by Limberger et al., (2018) assumed two fixed temperature boundary conditions:

- one deep boundary condition (600°C) in the magmatic chamber, of 9.5 km wide and 1.5 km high, below the caldera in the basement formation ;
- one atmospheric boundary condition (25°C) at the top surface of the model.

1.5.2 Geothermal flow

The conceptual model proposed by Arellano et al., (2003) consists of two geothermal reservoirs in Los Humeros field: a shallow liquid-dominant reservoir located between 1025 and 1600 m a.s.l. and a deeper vapour-dominated reservoir located between 100 and 850 m a.s.l with low liquid saturation. The reservoirs are separated by a low permeability vitric tuff (Toba Humeros). According to Cedillo Rodríguez, (2000) the temperature records (Torres-Rodriguez, 1993), the geochemistry of fluids (Tovar and López, 1998), petrophysics analysis (Viggiano and C., 1988) and geothermal wells in the field of Los Humeros all confirmed the presence of two reservoirs with different geothermal fluids.

However, studies by Carrasco-Núñez et al., (2017) and Gutiérrez-Negrín et al., (2010) put forward a single reservoir model since the impermeable tuff unit allegedly separating the reservoir is not observed in all wells in the caldera suggesting that the unit is discontinuous. According to their studies, geothermal wells are intercepting different feeding zones.

Figure 8 presents a temperature profile of wells located in the Los Humeros geothermal field. The values from CFE where corrected to account for deviated wells and due to non-equilibrium of some data using correction (ICS from Goutorbe et al., (2007)) which used the principal of return to equilibrium of bottom hole temperature through time.

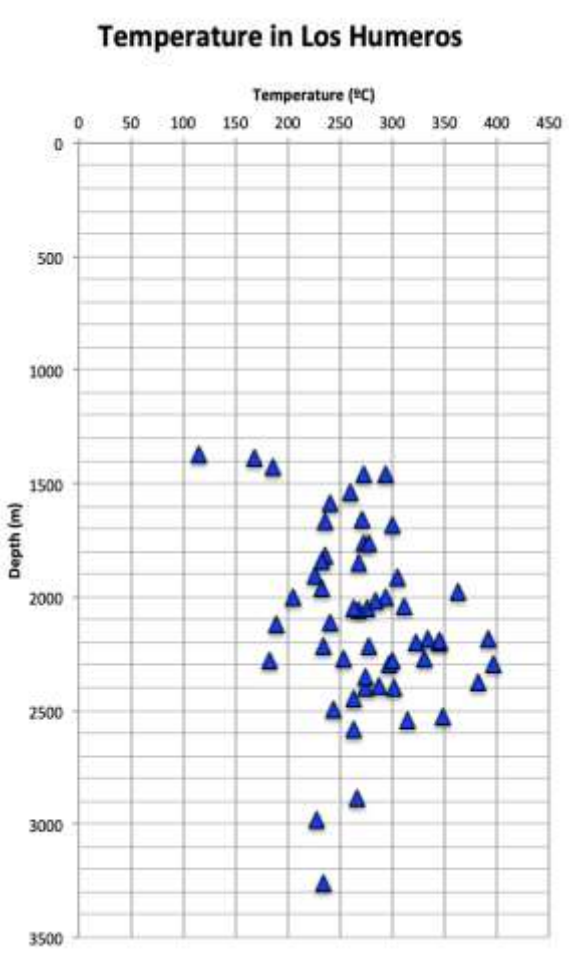

Figure 8: Temperature profile of 52 geothermal wells of Los Humeros geothermal field, corrected with deviation of wells and equilibrium state (Bonté, 2018)

2 Groundwater flow or Hydrothermal model of Los Humeros at the regional scale

2.1 3D Conceptual model

The first stage of numerical model generation is to build a conceptual model of Los Humeros. The conceptual model integrates the constraints (such as geologic, hydraulic and thermal characteristics) provided by the numerous studies (see section 1) into a 3D explanation of the geothermal system. In the following paragraph, we briefly recalled the main constraints, which are used to build the conceptual and then the numerical model.

Fluid flow in the LHGF is strongly influenced by faults and the associated fractures formed during the tectonic and volcanic episodes. Therefore, one of our major objective is to consider the influence of faults, which enable fluid flow and consequently impact hydrothermal processes and the global behavior of this geothermal system.

2.2 From the 3D geological model to 3D geometry

The 3D geological model used for this study is the preliminary 3D geological model resulting from Task 3.1 of the GEMex project.

Calcagno et al., (2019) built two geological models, based on the recent work of Carrasco-Núñez et al., (2017) and Norini et al., (2015). The cross section presented in Figure 10 were used to constrain the models, along with reinterpreted geological maps of the sites (Carrasco-Núñez et al. 2017). In addition, the Comisión Federal de Electricidad (CFE) has provided geological description of sixteen wells. One of the model was built at a local scale and focused on the geothermal target (9.5 km x 12.5 km x 12 km) while the second is define at a regional sale (56 km x 36 km x 12 km). The vertical extension is limited at the bottom of the model at 7 km below sea level.

The regional geological model from (Calcagno et al., 2018) considered for the present study is composed of **twelve faults inside the Los Humeros caldera rim, and four other faults outside** which derive from (López-Hernández, 1995). The Los Humeros caldera rim was modelled as a single closed shape delimiting the main volcanic structure. The modelled regional faults are: (1) Alchichica, (2) Antigua Fault, (3) Cueva Ahumada, (4) Cuyuaco, (5) El Limon Fault, (6) LH Caldera Rim, (7) LH Fault, (8) Los Potreros Caldera, (9) La Cuesta, (10) Las Cruces, (11) Las Papas, (12) Las Viboras, (13) Los Conejos, (14) Mastaloya Crater, (15) Mastaloya Fault, (16) Totolcingo (Figure 9). They belong to a fault network where: (3), (7), (9), (12), and (15) stop on (2).

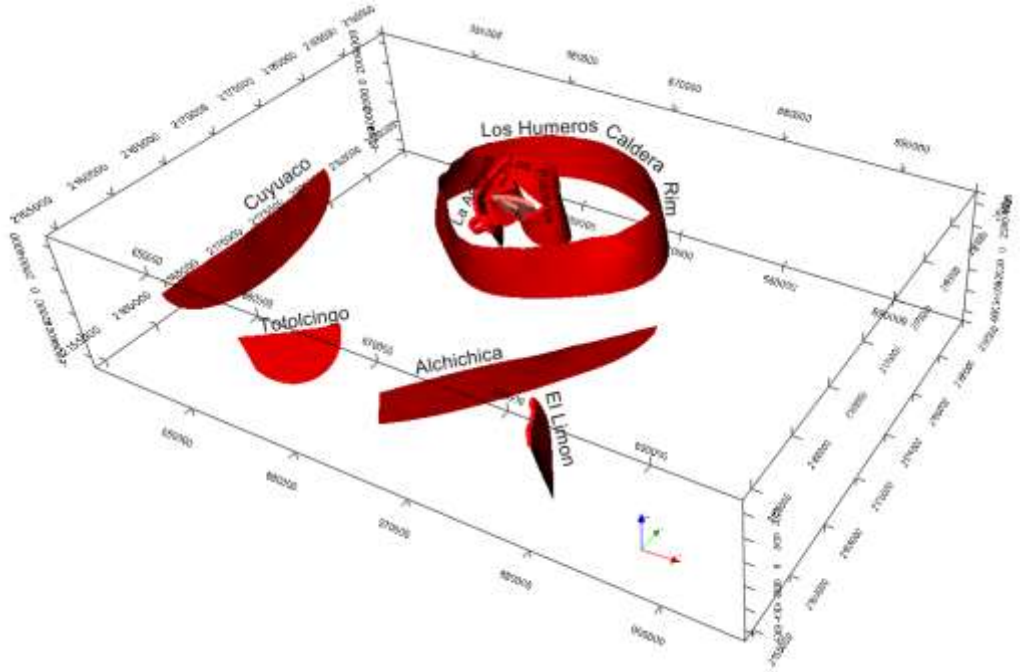

Figure 9: The Los Humeros regional fault model, including twelve faults inside the caldera rim and four outside (Calcagno et al, 2018)

Four groups of formations were considered in addition to the fault model to represent the geology of Los Humeros: **pre-volcanic basement, pre-caldera volcanism, caldera stage, and post-caldera volcanism** (see Table 1). The classification derives from the group proposed by (Carrasco-Núñez et al., 2017).

In addition to the existing data (map, two reference cross-sections, sixteen well logs) and where needed, eleven more cross-sections were interpreted for input into the model (as cross section in Figure 4).

The initial geological model at regional scale used in this study is presented in Figure 10. Considering the scale of the problem studied here, note that some simplifications are necessary (at least initially). Firstly, two geothermal reservoirs are identified in Los Humeros field (Arellano et al., 2003): a shallow liquid-dominant reservoir located between 1025 and 1600 m a.s.l. and a deeper one located between 100 and 850 m a.s.l. with low liquid saturation. They are separated by a low permeability vitric tuff (Toba Humeros). **In the geological model, the two reservoirs belong to the same formation of the pre-caldera group** (Figure 10) and have thus not been dissociated. Similarly, a high density of faults is localized within the caldera rim (twelve faults). Some of the smallest faults inside the LP caldera have not been considered and the dynamic numerical simulations were carried out with only eight faults out of the twelves modelled (Figure 11).

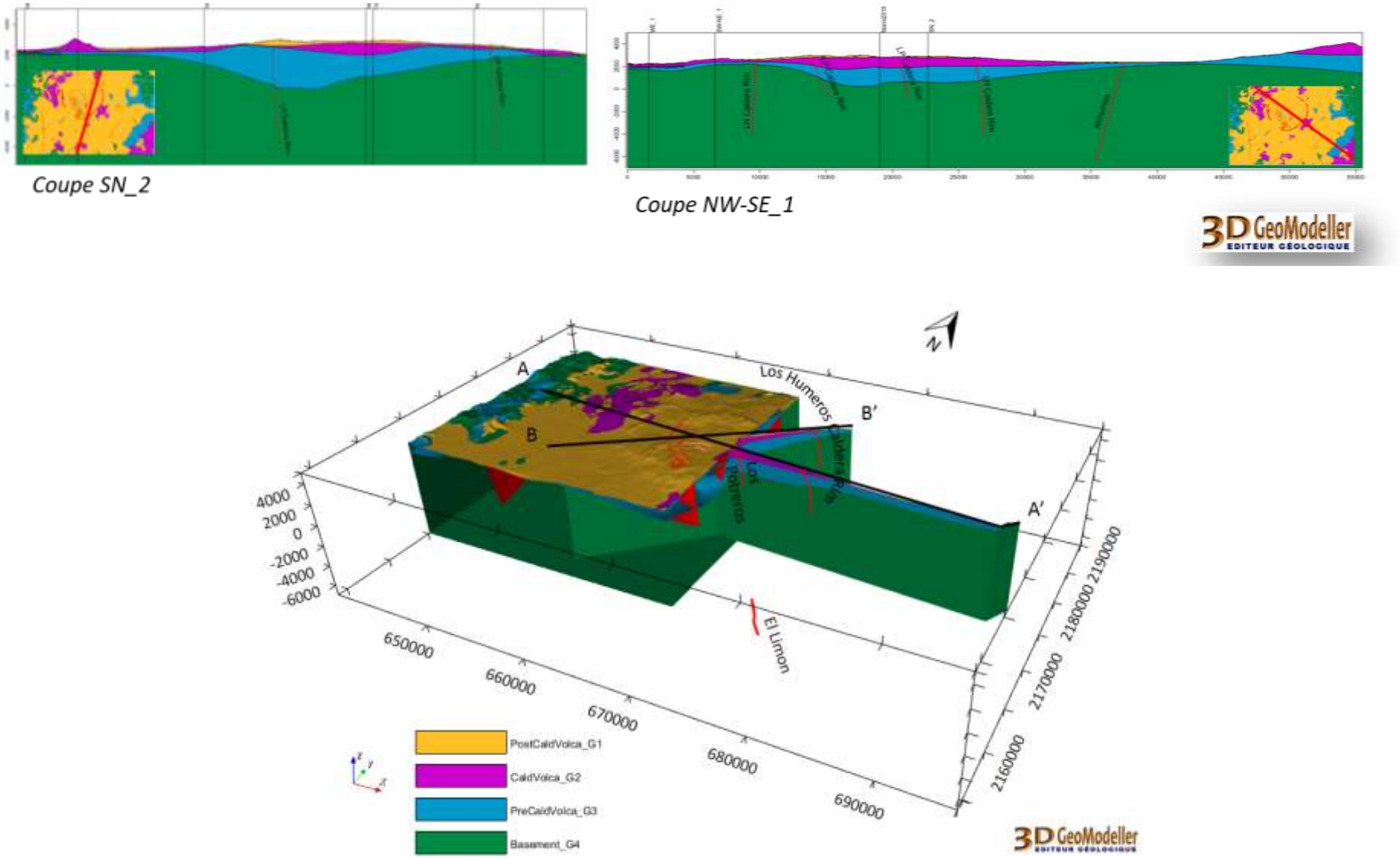

Figure 10: Cross section AB (top left) and CD (top right) from (Norini et al., 2015) and aerial view of the geological model at regional scale of LHVC with the four geological groups (bottom) from (Calcagno et al. 2018)

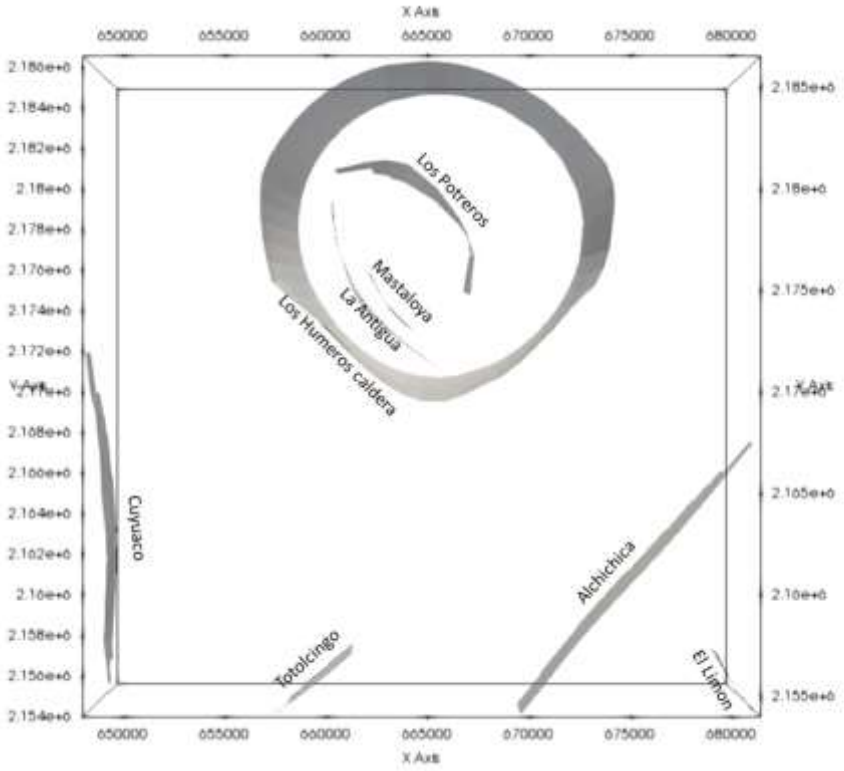

Figure 11: Faults defined in the hydrothermal regional model of Los Humeros

2.3 Permeability

As already mentioned, the Post-caldera contains shallow aquifers, the Caldera unit forms an aquitard and acts as a seal-cap, the Pre-caldera unit contains the geothermal fluids and the basement is expected to host superhot fluids (that may present secondary permeability).

Then according to these information the 3D geological model (composed of 4 main units and 8 faults) has been simplified as follows:

- The Post-Caldera and the Caldera are joined and considered as a unique unit in order to represent the cover. As a first approximation (and due to mesh resolution), this unit is considered relatively permeable. Thus, the effect of the clay cap at the top of the reservoir is not considered.
- The Pre-Caldera unit contains the geothermal fluids and represents the main reservoir. Indeed, the liquid-dominant reservoir located at around 1000 meters depth below the surface is considered as part of the Pre-Caldera andesite deposits.
- The Basement is composed of sedimentary deposits and crystalline metamorphic rocks.
- Faults are explicitly considered and act as conduit for fluid flow. As the faults can intersect any of the lithologies of the permeability model, the permeability of the fault must be treated with a special care (as function of the depth) in order to enable a positive contrast of permeability between the fault and the units.

Permeability measurements have been estimated through WP6.1 and have been considered for the conceptual permeability model. Granodiorite permeability has been estimated to 10^{-18} m² and reservoir formation to 10^{-14} m². These values has been used as the reference values to populate the numerical model (see section 3.3 and Table 4).

3 Hydrothermal numerical model of Los Humeros at the regional scale

Modelling a geothermal system (such as Los Humeros) requires the process of solving the equations of mass flow and heat through a fractured porous media. The simulation code used in this study is ComPASS.

3.1 ComPASS

ComPASS (Computing Parallel Architecture to Speed up Simulations) is a general purpose multiphase flow simulation platform adapted to geothermal simulation which is currently developed in the framework of the ANR (French National Research Agency) funded project CHARMS (ANR-16-CE06-0009) which spans 2017-2020. The main objective of the project is to achieve a code which is able to efficiently perform flow simulations on mesh discretization of complex geological models, without simplification of the underlying geological model. The main specifications are:

- to perform multiphase multicomponent thermal flow simulation on generic 3D unstructured meshes, possibly containing immersed intersecting fractures, without geometric discretization effects such as "grid orientation effects",
- to show good convergence behavior when solving the highly nonlinear physics of multiphase hydrothermal circulations,
- to achieve good scalability properties to take advantage of the multi-core and parallel architectures of current computers and benefit from the ever increasing availability of supercomputers,
- to accurately deal with the abrupt variations of petrophysical properties and distributions generated from geostatistical techniques, including aperture/permeability distributions along fault/fracture surfaces,
- include the possibility to specify a wide range of boundary conditions with complementary conditions with a special focus on the modeling of shallow processes (shallow processes in the vadose zone),
- accurately describe transport phenomena (heat and tracer) in an eulerian framework.

The reader interested in further details is referred to the bibliography, namely the works by Xing et al. (Xing et al., 2017a) for the description of the theoretical and numerical aspects of the modeling of compositional multiphase flows in fractured media, Beaude et al. for the integration of complex well architectures (Beaude et al., 2017a) and the specification of complex boundary conditions (Beaude et al., 2017b, 2018). A conference proceedings to the Stanford Geothermal Workshop by Lopez *et al.* (2018) summarizes most of this material. Additional information is also available from the CHARMS website (http://www.anr-charms.org). ComPASS is open sourced under GPL v.3 and can be freely accessed upon request[2].

Xing *et al.* (Xing et al., 2017) detailed the generic formulation of the compositional model currently implemented in ComPASS, which is based on a Coats' type formulation (Coats, 1989) and extends the work by Eymard *et al.* (2012) to non-isothermal flows. It accounts for an arbitrary nonzero number of components in each phase allowing to model immiscible, partially miscible or fully miscible flows. ComPASS can already be used to performed simulation with various simple physics (e.g. diphasic pure water) but the code is still in active development phase (cf. chapter 5).

As concerns the porous medium discretization, two classes of models, dual continuum and discrete fracture models, are typically employed and possibly coupled to simulate flow and transport in fractured porous media. Dual continuum models assume that the fracture network is well connected and can be homogenized as a

[2] following the procedure detailed at http://www.anr-charms.org/page/compass-code#get-involved

continuum coupled to the matrix continuum using transfer functions (*e.g.* the MINC approach in TOUGH2 (Pruess, 1992)). On the other hand, discrete fracture models (DFM), represent explicitly the fractures as co-dimension one surfaces immersed in the surrounding matrix domain.

ComPASS uses the DFM approach with a lower dimension physical model along the fracture, which is derived from the full three-dimensional model by integration and averaging along the – possibly variable - width of each fracture. The resulting so-called hybrid-dimensional model couples the 3D model in the matrix with a 2D model in the fracture network taking into account the jump of the normal fluxes as well as additional transmission conditions at the matrix fracture interfaces. These transmission conditions depend on the mathematical model and on additional physical assumptions depending on the fracture behavior (drain vs. barrier).

Mass transfers are computed using generalized Darcy velocities for each phase and involve the phase relative permeabilities, dynamic viscosities and the rock intrinsic permeability tensor. Energy fluxes are obtained as the sum of an advective component related to the enthalpies of the phases advected by the aforementioned phase Darcy velocities and a diffusive component given by the Fourier law and involving the rock bulk thermal conductivity. This lead to a system of conservation equations is coupled to closure laws consisting of component mass balance and phase volume balance as well as thermodynamical equilibrium for each component present in at least two phases among the set of present phases.

Over the last few years, much progress has been made in the consistent and robust discretization of diffusion processes in porous media involved in Darcy and Fourier fluxes. These research efforts resulted in several numerical schemes designed with a sound mathematical framework and able to deal with subsurface spatial heterogeneities (permeability variations, anisotropies…) and general polyhedral meshes. ComPASS currently implements the Vertex Approximate Gradient (VAG) finite volume scheme (Eymard et al., 2012) which belongs to a broader family of numerical scheme called Gradient Schemes (Droniou et al., 2016). The VAG discretization of hybrid-dimensional two-phase Darcy flows was introduced by Brenner *et al.* (2016) and generalized to multiphase multicomponent flow by Xing *et al.* (Xing et al., 2017). It considers generalised polyhedral meshes of the simulation domain, which are assumed conforming. The cells are star-shapped polyhedrons, and faces are not necessarily planar in the sense that they can be defined as the union of triangles joining the edges of the face to a so-called *face centre*.

The VAG scheme is a Control Volume scheme in the sense that it results, for each non Dirichlet degree of freedom, in a molar or energy balance equation. The construction of the control volumes at each degree of freedom is based on partitions of the cells and of the fracture faces: cell (resp. fracture face) volumes are splitted between the cell (resp. fracture face) center and its boundary nodes. As shown in Brenner et al. (2015), the flexibility in the choice of the control volumes is a crucial asset, compared with usual Control Volume Finite Element Methods (CVFE) approaches and allows to significantly improve the accuracy of the scheme when the permeability field is highly heterogeneous. Figure 12, also shows that, as opposed to usual CVFE approaches, this flexibility allows to define the control volumes in the fractures with no contribution from the matrix in order to avoid the artificial enlargement of the flow path in the fractures thus limiting numerical diffusion.

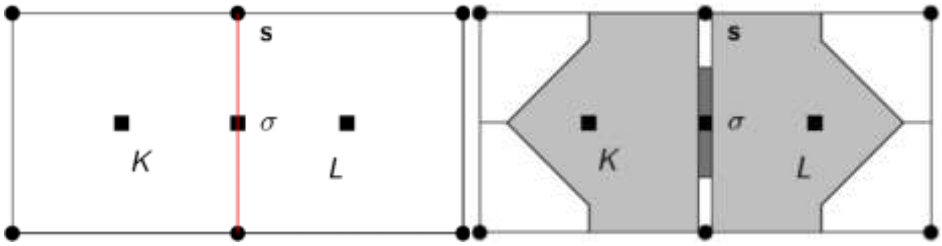

Figure 12: On the left: two cells (K and L) splitted by one fracture face (in red). On the right: example of control volumes associated with the two cells centers (light grey) and with the fracture face center (dark grey) and with (matrix and fracture) nodes (in white). The width of the fracture is enlarged for the sake of clarity.

Moreover, to avoid too small control volumes at the nodes located at the fracture intersection, all the fracture faces containing such a node share their volume with it. It results that the control volumes at the fracture intersection nodes are not smaller than at any other fracture degrees of freedom.

The time discretization is based on a fully implicit Euler scheme to avoid severe restrictions on the time steps due to the small volumes and high velocities in the fractures. A phase based upwind scheme is used for the approximation of the mobilities in the Darcy fluxes. (1)

The resulting non-linear system is solved by a specific parallel implementation of the active set Newton-Raphson algorithm (e.g. Coats, 1989) which is detailed by Xing *et al.* (Xing et al., 2017). Specific features of the VAG scheme make that two successive elimination steps considerably reduce the size of the linear system to be solved for each Newton-Raphson iteration, making the ComPASS implementation of the VAG scheme an essentially nodal scheme. It is consequently very efficient on meshes composed mainly of tetrahedrons which have much more cells than nodes.

Finally, the resulting ill conditioned linear system involved in each Newton-Raphson iteration is solved using an iterative solver (typically GMRES) combined with a state-of-the-art preconditioner adapted to the elliptic or parabolic nature of the pressure unknown and to the coupling with the remaining hyperbolic or parabolic unknowns.

Results from ComPASS were visualized and explored using the open source Paraview tool (https://www.paraview.org/) using the post-process script provided along with ComPASS.

3.2 Mesh generation from geological model

To apply numerical resolution on the model, it is necessary to discretize explicitly and build mesh model. The mesh wills then ben populated with parameters before completing numerical simulation. To that purpose, both surface and volumes need to be discretized.

Methods based on the implicit description of geometrical objects, as those implemented in GeoModeller (Calcagno et al., 2008; Lajaunie et al., 1997), offer an efficient framework to quickly build complex structural models with the occurrence of faults and fractures. One of the key aspects is that these methods can be entirely parametrized and do not require manual interaction, like so-called explicit/constructive methods (Collon and Caumon, 2017). This makes implicit modeling methods particularly well suited for sensitivity studies and the quantitative analysis of uncertainties associated with 3D geological models (e.g. de la Varga et al., 2015; Wellmann et al., 2012, 2014).

Yet, when it comes to produce conforming meshes of such complex geological models in order to run dynamic simulations, the implicit nature of surfaces make volume meshing a non-trivial task. Corner-point grids are

widely used in the industry but rely on the sampling of the geological models and generate important approximations of the geometries. State of the art meshing algorithms essentially rely on tetrahedral meshes produced with various algorithms. Most of these algorithms need as input a Boundary Representation (*B-Rep*) of the geological model. This *B-Rep* needs to be clean, sealed and topologically consistent with the geological model (e.g. Caumon *et al.* (2004)). These boundaries define connected components, which are subdivided into smaller polyhedral by the meshing algorithm.

The Computational Geometry Algorithms Library (CGAL) is an open source project delivering algorithms for geometric computation in various areas (https://www.cgal.org/). It provides a powerful 3D mesh generation package[3] dedicated to implicit frameworks. It does not explicitly require a B-Rep of the model but rather reconstructs it from two simple spatial predicates. Courrioux et al. (2012) implemented the use of this framework into the GeoModeller software, thus giving the possibility to produce conforming tetrahedral meshes out of any geological model that correctly discretize 2D geometrical boundaries (geological interfaces, faults…) or 1D sharp features (surfaces intersection, well paths…).

Yet, this implementation, which has been used in the framework of the GEMex still suffers some flaws to be directly used for dynamic flow modelling:

- the approximate handling of the boundaries location and their intersection can generate the accumulation of small tetrahedras in parts of the mesh,
- the Delaunay refinement (Rineau and Yvinec, 2007) used in the mesh generation process produces several cells with high aspect ratio (bad quality cells),
- the resulting mesh is isotropic which leads to a large number of cells in the case of the discretization of geological bodies such as multilayer aquifers with a low thickness to width ratio.

The latest of these drawbacks is not such a problem as ComPASS is a massively parallel code but it can lead to have very big simulation to achieve an acceptable vertical resolution. The other two are of major concern as very small of bad quality cells with diphasic flows typically lead to computation time steps collapsing to very small values resulting in intractable simulations.

One workaround implemented during the GEMex project to constrain cells size and limits between formations was to fall back to more classical way of meshing multilayers model, with the vertical extrusion of a triangle mesh of the topography, thus producing an unstructured mesh with triangle-based prismatic cells. Consequently, prisms are vertical and some information about the initial surfaces shape was lost to be able to match the contour of prisms. The major consequence was that faults were considered to be sub-vertical and a new version of the geological model, modified accordingly, was used. Figure 13 displays the discontinuous aspect of limits between formations. The same phenomenon is observed for the faults contours. The approximation made is considered as acceptable with respect to the gain obtained in terms of computation time.

[3] https://doc.cgal.org/latest/Mesh_3/index.html

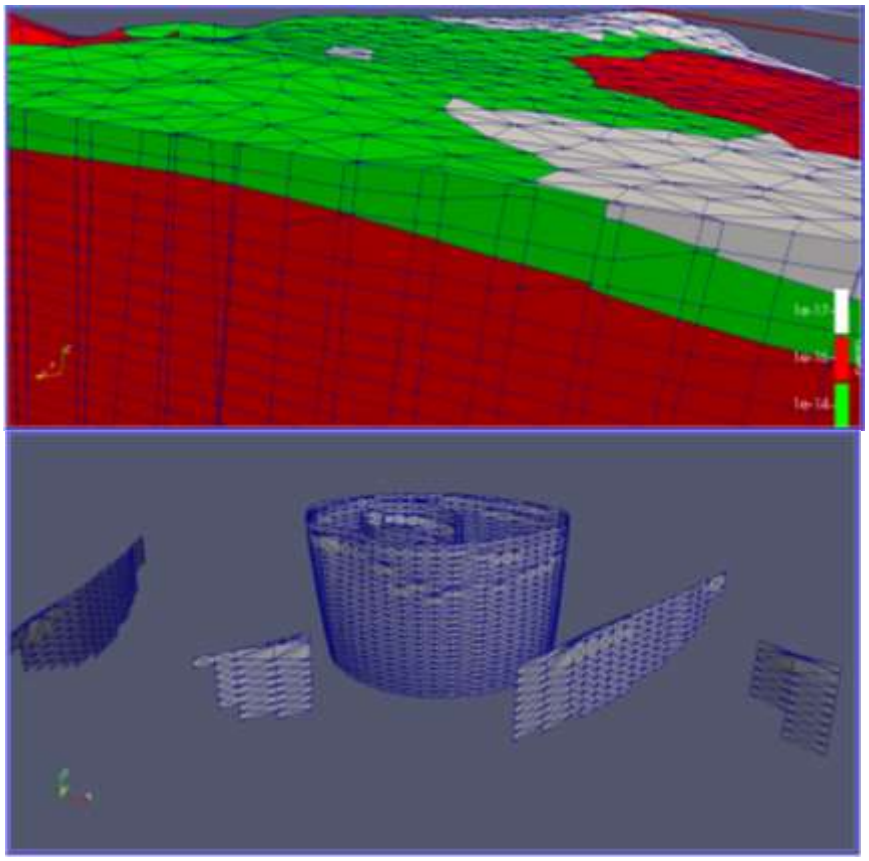

Figure 13: Aspect of the prismatic mesh generated from an extrusion of a triangulated surface.

The **mesh used for simulations contains 53304 prisms (137197 faces, 29575 nodes, 1486 frac)** and is relatively easy to manage. Sensitivity run and simulations could be carried out with respect of differences between formations (especially in terms of permeability distribution). With the prismatic mesh, it is important to take into account that facets are either triangles or quadrilaterals and thus, managing these data will be slightly different. A first step is to confirm how both shape are distributed inside the mesh by sorting out triangulated facets from quadratic ones. Visualization can them be done in Paraview. All quadratic facets are vertical, and their bases are connected with triangulated surfaces, that are sub-horizontal.

Based on this generated mesh, information about vertices, facets and cells are extracted with a general python method, that also gives a list of tags for the facets in order to identify their belonging to a given geological formation and relation to borders or faults as explained in Table 3. The tags information is provided in a text file generated along with the mesh which is stored in ASCII (prisms) or binary file (tetrahedral meshes generated with CGAL).

Table 3: Structures extracted from the geological model and the associated tags

Borders	Borders tags	Faults	Faults tags	Formations	Formation tags
Zmax	-1	Alchichica	1	Basement_G4	1
Zmin	-2	AntiguaFault	2	PreCaldVolca_G3	2
Xmin	-3	Cuyuaco	3	CaldVolca_G2	3
Xmax	-4	ElLimonFault	4	PostCaldVolca_G1	4
Ymin	-5	LHCaldRim	5		
Ymax	-6	LPotretosCald	6		
		Totolcingo	7		

3.3 Hydraulic and thermal properties implemented

The **distribution of the permeability** is done in accordance with the definition of tags (based on the units of the 3D geological model) and the permeability defined in the conceptual model. Figure 14 presents the distribution of the permeability for the three groups of formations (geological units) considered in this study.

Similarly, a permeability is assigned to the faults which are considered as permeable and act as conduit for fluid flow. As the faults intersect any of the lithology of the permeability model, the permeability of the fault decreases with depth. Moreover, in order to ensure the drain behaviour of the faults, the property distribution is assigned so that fault permeability is greater than the one of the surrounding matrix. Figure 15 presents the distribution of the permeability assigned to the faults. Table 4 summarizes the value of hydraulic and thermal properties assigned to each formations. Note that in this study and as a first approximation, the thermal conductivity is in average 2 W/mK for all the units.

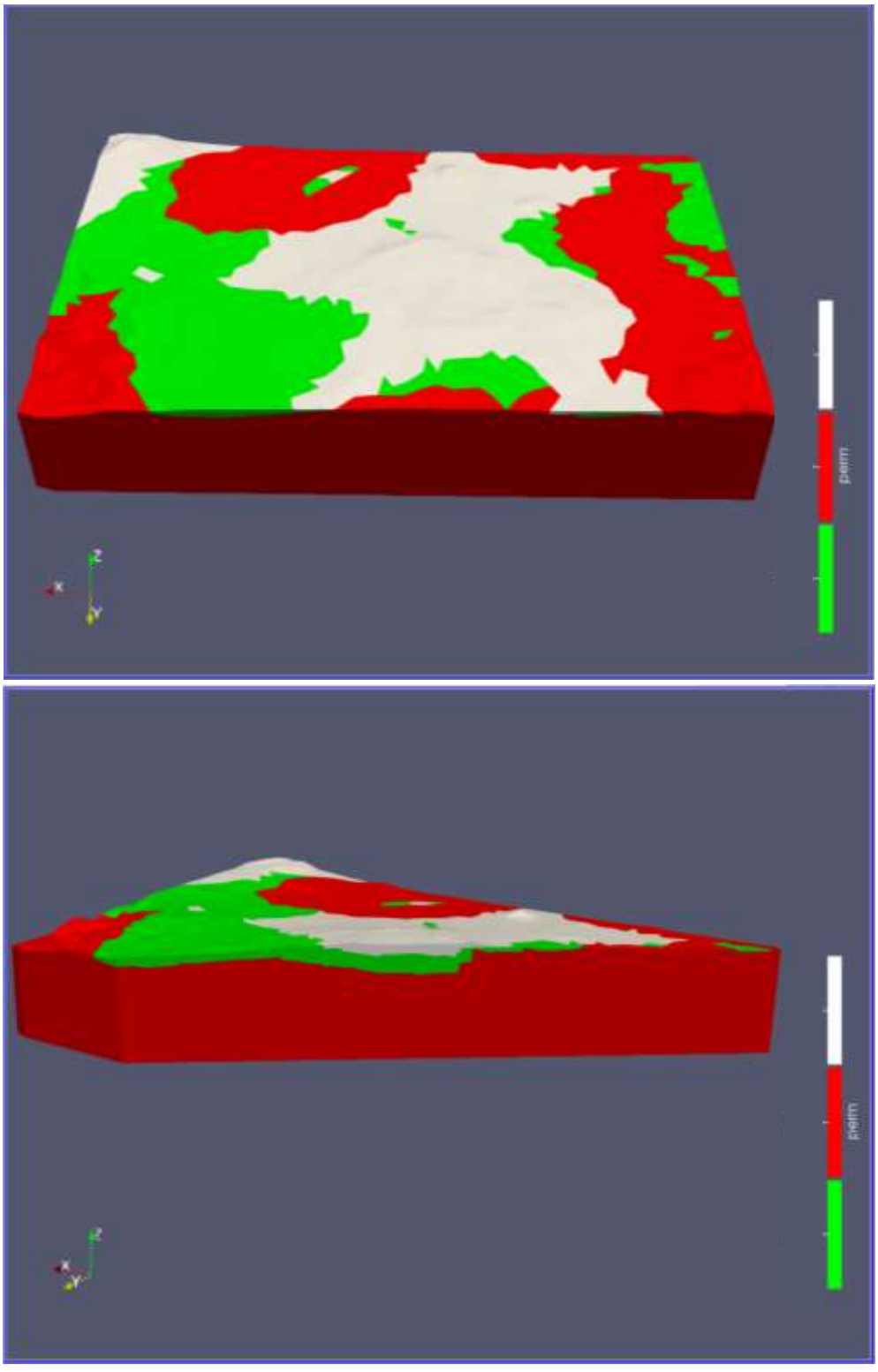

Figure 14: Distribution of permeability within the numerical model in accordance with the geological units. At the top: View from above and at the bottom: Cross-section (NE-SW) through the center of the caldera of Los Humeros.

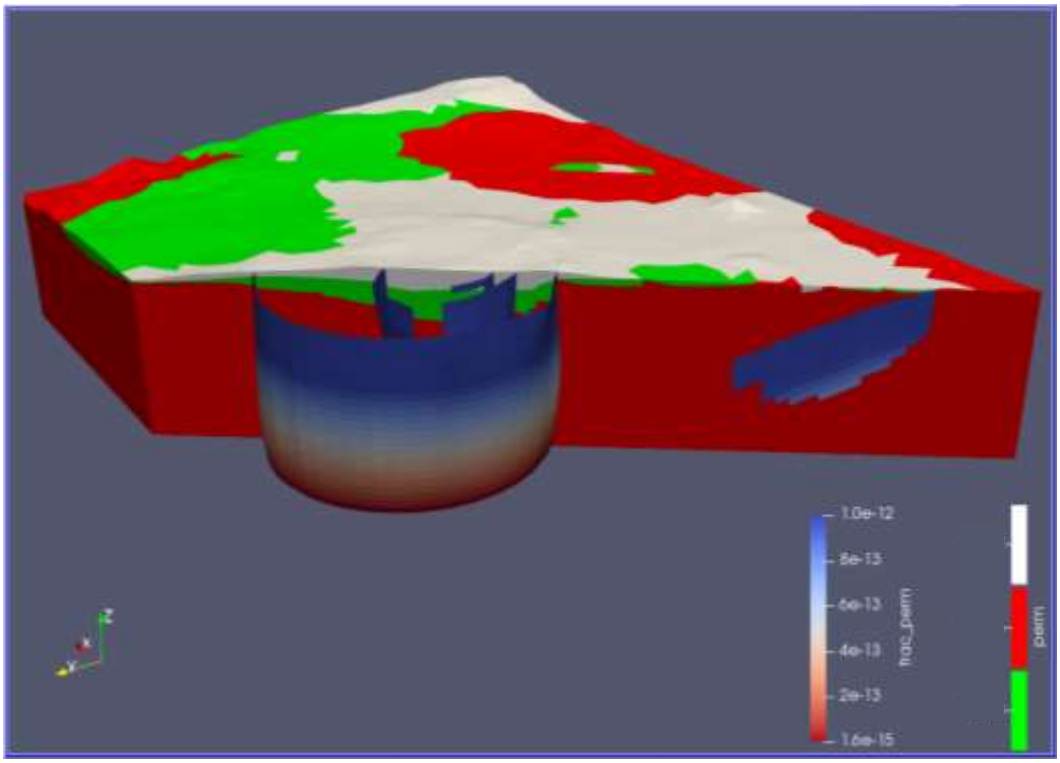

Figure 15: Distribution of permeability for the faults as function of depth

Petrophysical rock properties resulting from WP6.1 work have been considered for the conceptual permeability model.

Table 4: Hydraulic and thermal properties for each group of formations considered in the numerical model

Formations	Color	Permeability (m^2)	Porosity	Thermal conductivity ($W.m^{-1}.K^{-1}$)
Basement_G4		1E-18	0.15	2
PreCaldVolca_G3		1E-14	0.15	2
CaldVolca_G2 & PostCaldVolca_G1		1E-14	0.15	2
Faults		Function of depth K=f(z)	0.5	2

3.4 Initial and boundary conditions

Constant values of physical states have to be set so that the solution can converge. Dirichlet nodes are vertices where we set constant values and Neumann faces are facets where we set constant fluxes (heat or mass).

3.4.1 Boundary conditions

3.4.1.1 Dirichlet

Here, Dirichlet nodes correspond to the topography, where atmospheric pressure and temperature are fixed and constant.

Then at the top boundary (surface) of the model, along the vertices, the pressure is equal to **one atmosphere and the temperature is fixed at 20°C**. The North, South, East, West boundaries (sides) and the bottom boundary corresponds to **no-flow boundary condition**.

3.4.1.2 Neumann

Constant heat fluxes are imposed on faces at the bottom boundary. A **global heat flux of 0.05 W/m^2** (issued from the study of Limberger et al., (2018)) is set on every bottom facets. **An additional heat flux on facets within the caldera** is applied through the definition of a cylinder representing the magmatic chamber. This additional flux decreases exponentially outside the cylinder. Note that the power of the additional flux imposed at the base of the model constitutes one of the parameter (boundary condition) investigated through the numerical study presented here (see section 4.3). A **molar fluxes (1.10^{-7} kg/s)** can be set on every top facets to represent precipitation that occur in this area (Jimenez-Salgado, 2014).

3.4.2 Initial states

Initial temperature and pressure are set as a linear function of depth. We use the mean **geothermal gradient on Earth and hydrostatic pressure**: 0.03 °C.m^{-1} and 0.1 bar.m^{-1} respectively.

3.4.3 Tested parameters

Numerous sensitive and uncertain parameters can be identified when performing hydro-geothermal numerical simulations. Over the regional model of Los Humeros, matrix permeability, fracture permeability, heat source flux and global flux, mesh distribution and geometry have been identified as the main parameters impacting heat transfer and fluid flow.

Matrix and fracture permeability are sensitive parameters in the model as they govern pressure and fluid flow in the reservoir and influence heat and mass transfer over the model. As presented in section 3.3, faults are considered to be permeable conduits and participate actively in flow and heat transport. Different configuration were tested to identify the impact of fault permeability variation with depth. The principal sensitivities carried out regarding formation permeability considered either a two layer model with high contrast in permeability between the Basement formation and higher permeability layers of the Caldera and Pre-Caldera formations or a multilayer permeability distribution with contrast between all three formations represented in the model (see Table 4.).

Heat flux in the model and below the caldera and its influence over mass flow in the reservoir and basement have been appreciated through sensitivity simulations. Despite variations over flow path in the deeper part of the caldera, the influence of boundary conditions at surface seems to screen important variation of temperature

in the caldera. Improvement to constrain the model is required to fully appreciation the impact of heat flux values over temperature (see section 5).

The **definition and geometry of meshes** are key parameters in numerical simulation. Indeed, the influence on flux have been appreciated using either prismatic or tetrahedral meshes over the regional model of Los Humeros for similar geological and fault structures.

4 Results of the simulations

One of the objective of this study is to simulate the natural state (heat and mass flow) of the geothermal system at the regional scale while considering the key effects of faults on hydrothermal processes.

The main aim of this study focuses on the influence of main hydrological parameters (permeability of units and boundary conditions) on the distribution of flow and heat at the regional scale as described in section 3.4.3.

4.1 Global distribution of groundwater flow

Fluid flows are compartmentalized between the shallow formation of Post-Caldera, Caldera and Pre-Caldera on the one hand and the deeper Basement formation. The behaviour of the geothermal reservoir and in the Basement are analysed in the following section 4.1.1 and 4.1.2 respectively.

4.1.1 Groundwater flow in the shallower part

The geothermal target currently exploited by CFE in Los Humeros is located in the Pre-Caldera volcanic formation. As presented in Figure 16, the formation vertical extension reaches a maximum, below the caldera, at around -500 meters above sea level.

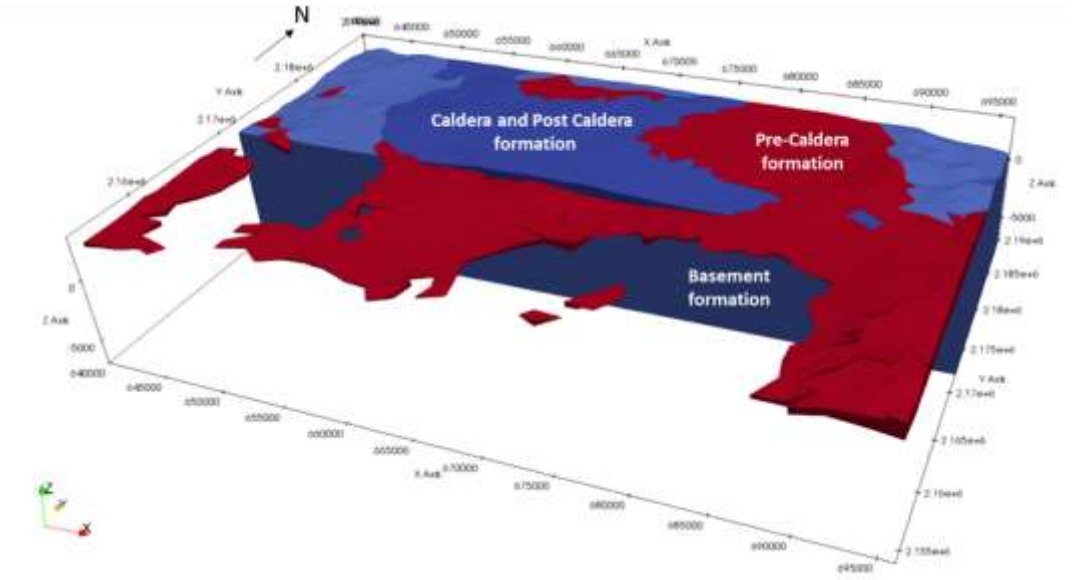

Figure 16: Formations defined in the model and highlight of the Pre-Caldera formation and its vertical extension

Figure 17 presents the simulated mass flux in the shallower portion of the model. While inside the caldera of LP the flux is oriented toward the SW, the flux in LH caldera -north from Los Potreros Rim- the flux is oriented toward the NE. The flux directly outside the caldera is radial.

Dirichlet boundary condition are imposed, with constant temperature and pressure, along the surface constrained by topography. Figure 18 presents the head map and MNT of Los Humeros overlapped to simulated mass flux in the reservoirs formation. As represented, highest points in the grip of the regional model correspond to starting point of flow streamline (so-called recharge areas). The Cuyaco, Totolcingo and Alchichica faults, south of the model, are low points where flow lines tends to outflow (so-called discharge areas). The consistent between the head map and simulated mass flux is limited and can be explained by the constrained imposed (initial and boundary conditions).

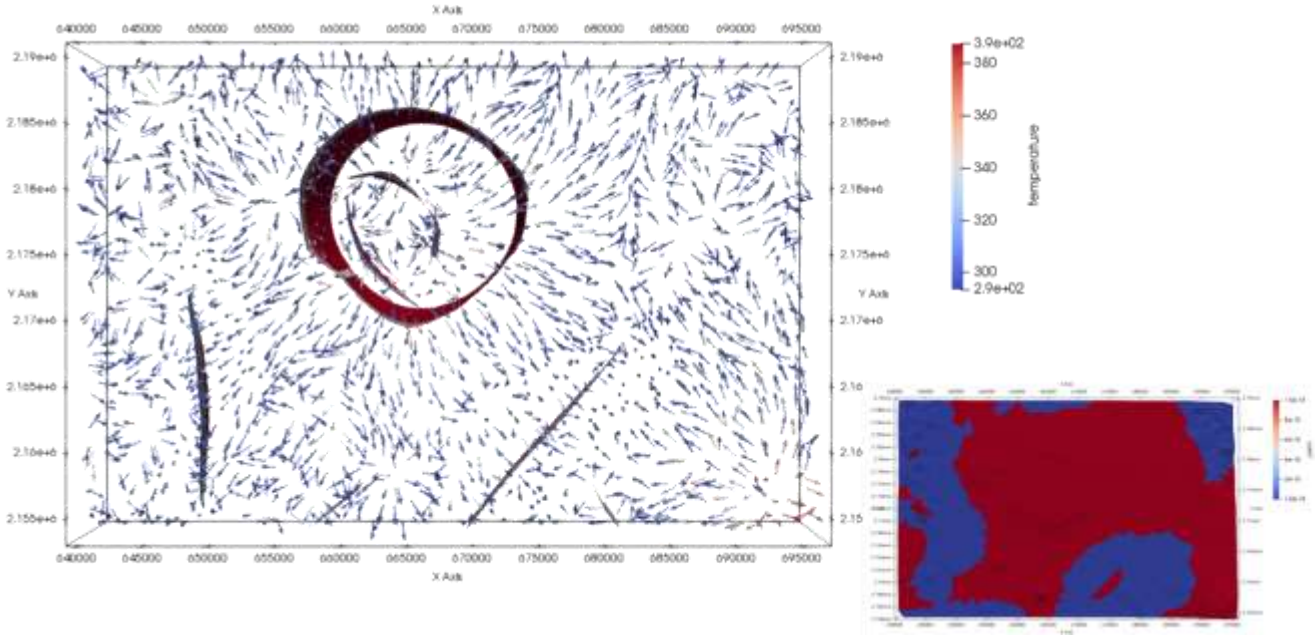

Figure 17: Simulated mass flux orientation unscaled and colored with temperature (K) over the regional model for permeability of 1.10^{-14} m² in the Caldera and Pre-Caldera formation using a prismatic mesh

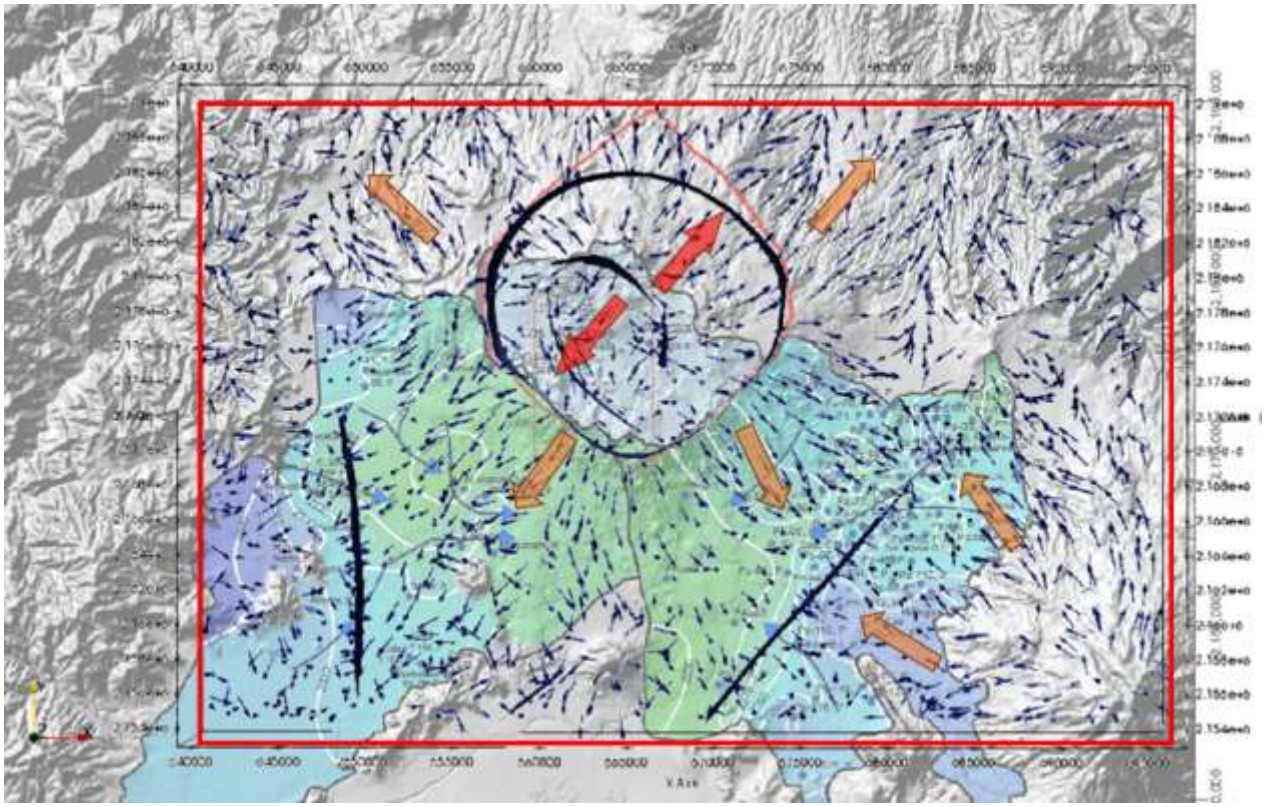

Figure 18: Water head map (Jimenez-Salgado, 2014) superimposed with simulated mass flux in the shallower part of the model using permeability of 1.10^{-14} m² in the Pre-Caldera and Caldera formation and with prismatic meshing. Extension of the model overlapped in red rectangle.

When looking at a cross section of mass flux in the shallow part of the model *i.e.* the reservoir formation participating in geothermal fluid production in LHVS as illustrated in Figure 19, one can rapidly identify the inflow and outflow of heat inside the calderas. The outflows are located in majority near the Los Humeros NE

Rim and the SW rim of Los Potreros calderas: La Antigua Fault (see Figure 11). The inflow zone are located in the NE rim of Los Potreros caldera. On both sides of LH caldera rim, the flux is outwardly oriented. The fluid is thus conducted along the Los Potreros North-Est rim of the caldera to the deeper area of the caldera and is heated through the influence of heat flux source in the basement of the model. The geothermal fluid is then conducted toward the shallow level of the reservoir along the faults of La Antigua in the center of LP caldera and along Los Humeros caldera rim.

The results obtained with simulation are thus consistent with the conclusion of the conceptual model introduced by (Norini et al., 2015) as presented in Figure 7Figure 9.

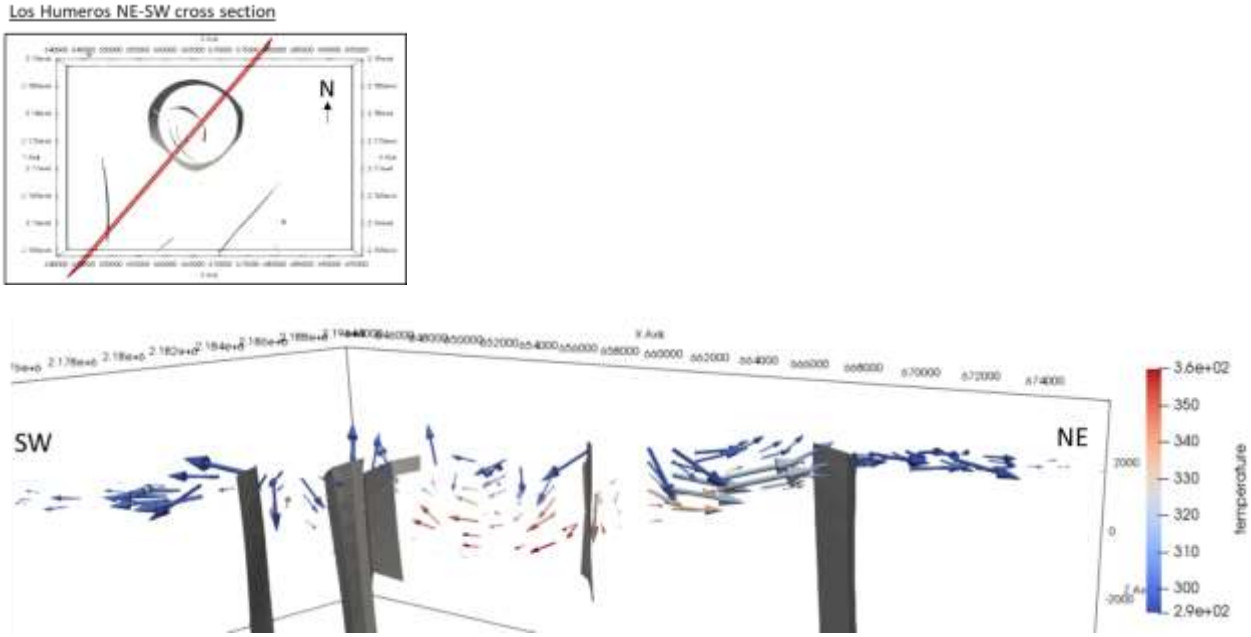

Figure 19: Orientation of simulated mass flux mapped with temperature (K), centered on LH and LP calderas along a NE-SW cross section using permeability of 1.10^{-14} m² in the permeable Pre-Caldera and Caldera formation and with prismatic meshing

4.1.2 Groundwater flow in the deeper part

An overview of the groundwater flow that occurred in the deeper part of the model is provided in the present section. Heat flux boundary condition are imposed at the bottom boundary of the model: below the caldera (0.1W/m²) and outside (0.05 W/m² for the remainder of the model boundary).

Figure 20 presents the mass flux orientation in the deeper part of the model (below 0 meter above sea level). Overall, upward mass flux can be observed in the deeper part (as shown in the NE-SW cross-section, see Figure 21). These upward mass fluxes tended to become more lateral in the shallower part. Note that the mass flux are mainly directed radially outwards and upwards (from the LH caldera inside to outside: see orange arrows). Outside the caldera two main flow directions can be observed: in the eastern part, the flow is mainly SW-NE (see purple arrow) and in the western part the flow is mainly SE-NW (see green arrow). To finish, inside the caldera, mainly upward flows occur (yellow arrow).

A detailed description of the simulated mass flux is provided by Figure 21, which shows the simulated mass flux orientation and temperature contour below 0 meter above sea level over a NE-SW cross section. The arrows (mass flux) show upward flows in the deeper part (as described in the previous paragraph) and highlight the impact of the powerful heat source below the caldera which strongly impacts the mass flux around the caldera.

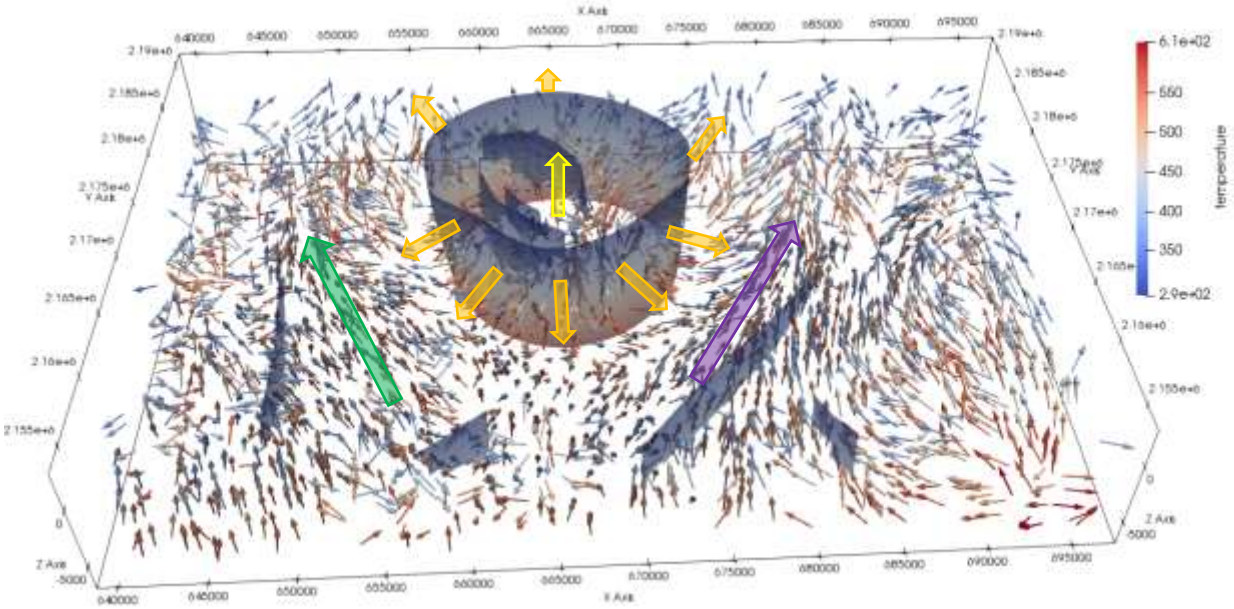

Figure 20: Simulated mass flux orientation in the deeper part of the model (below 0 meter above sea level), unscaled and colored with temperature (K) over the regional model, for permeability of 1.10^{-14} m² in the Caldera and Pre-Caldera formation and of 1.10^{-18} m² in the basement using a prismatic mesh

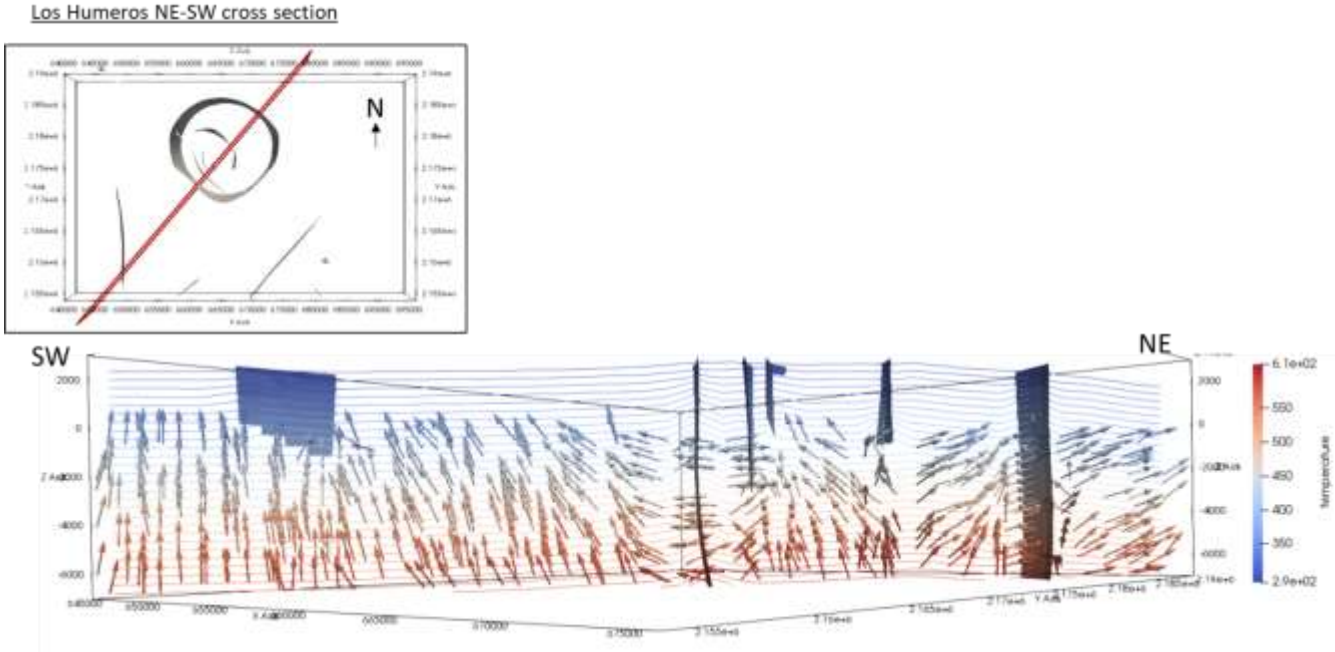

Figure 21: Simulated mass flux orientation and temperature (K) contour below 0 meter above sea level over a NE-SW cross section using permeability of 1.10-14 m² in the permeable Pre-Caldera and Caldera formation and 1.10-18m² in the matrix of the basement formation using a prismatic mesh

When looking at the flow occurring inside the calderas of LH and LP as depicted by Figure 22, two preferential heat paths can be observed as represented by (superimposed) red arrows. These preferential paths described a possible concentration of heat at the base of the La Antigua and Mastaloya faults (at the SW, see location in Figure 11) and a heat concentration between LP and LH calderas. These results are in accordance with the

study proposed by Norini et al., (2015), (see Figure 7). Nevertheless, this figure providing the temperature contours shows that the simulated temperature is lower than the measured.

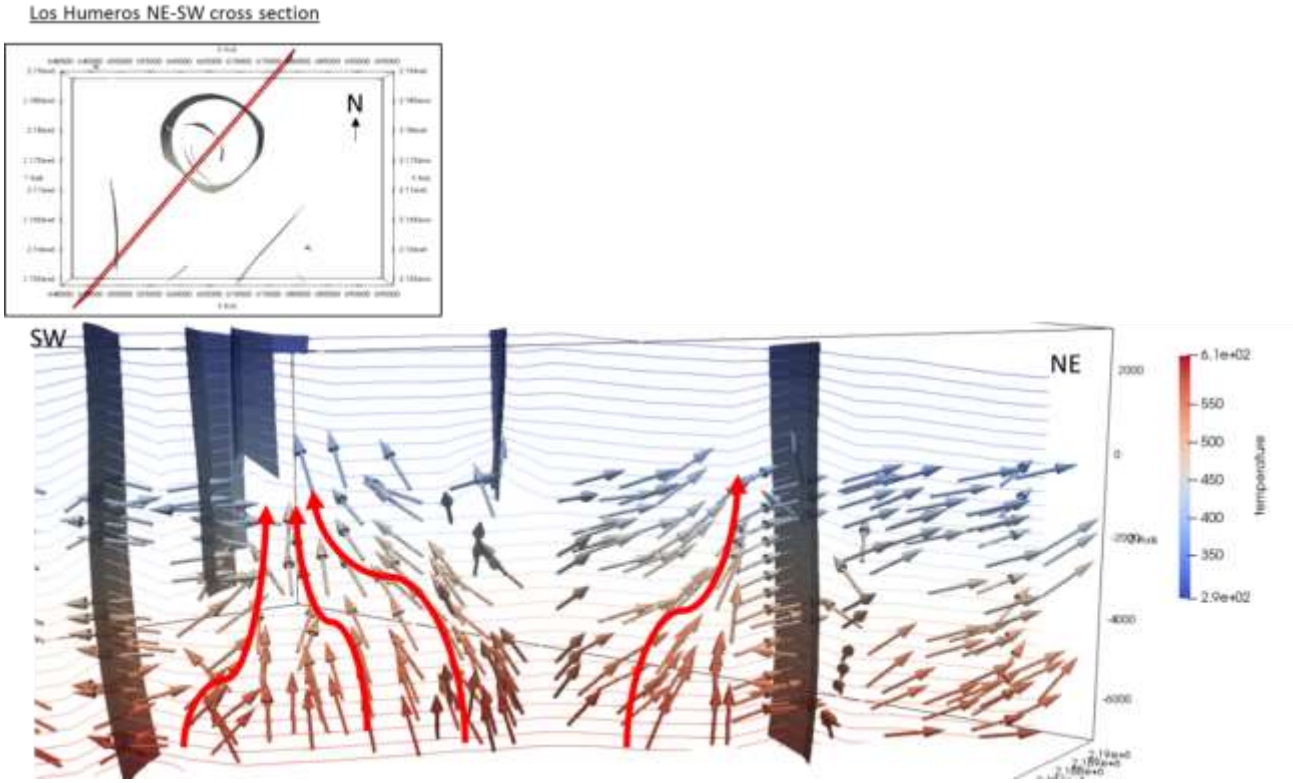

Figure 22: Zoom over the LH and LP calderas of simulated mass flux orientation and temperature contour (K) below 0 meter above sea level over a NE-SW cross section and schematic preferential heat path in the basement formation (red superimposition)

4.1.3 Results vs hydrogeochemistry evidences

From geochemical work carried out in GeMex, it is suggested that water collected from Los Humeros wells are mainly constituted of shallow water and small inflow of high-temperature deep water. These results seem in accordance with the numerical simulations that suggest a compartmentalization between the upper and the deeper part (Figure 19 vs Figure 21 and Figure 22). The fluxes in the upper part (where the wells are located) are mainly characterized by local groundwater loops (Figure 19) and a contribution (upward fluxes) from the deep part can be observed (Figure 21 and Figure 22). Note that the magnitude of fluxes are higher in the upper part (local loops) than the upward fluxes originating from the deeper part.

Second, the gas study suggests the presence of convection along permeable faults and the existence of links between deep geothermal reservoirs and subsurface fractures and faults. The most permeable zone when considering soil degassing is located in SW area and extends towards the N and NE. The numerical results seem to reflect these geochemistry evidences. Two preferential heat paths can be observed (Figure 22), which described a possible concentration of heat at the base of the La Antigua and Mastaloya faults (at the SW) and a heat concentration between LP and LH calderas (at the NW). Note that, these preferential paths and the concentration of fluxes are oriented towards faults.

Third, fluid-rock interaction in LH have also been studied through GeMex project (WP4). The main results indicate that infiltrated water may react with intersected formation before reaching the reservoir. The results of the numerical simulations suggest (as seen in Figure 19) that the inflow zone are located in the NE rim of

Los Potreros caldera. The fluid is thus conducted along the Los Potreros North-Est rim of the caldera to the deeper area of the caldera. Then the geothermal fluid is conducted toward the shallow level of the reservoir along the faults of La Antigua in the center of LP caldera and along Los Humeros caldera rim. Thus, these results (groundwater loops occuring within faults crossing several units) are consistent with the findings of the fluid-rock interaction studies.

4.2 Permeability distribution

The second analysis conducted in this study focuses on the permeability distribution within the regional model. Two different cases are presented and are related to the model presented in the previous section (3.3). Here, the influence of permeability variation is first tested in the Caldera and then in the Basement formation.

Figure 23 presents the results of sensitivity simulation regarding the influence of permeability variation in the Caldera formation (cover and seal cap). The total max flux orientation in the shallower part of the model for two different values of Caldera permeabilities was explored: $K_{caldera}=1.10^{-14}$ m² and $K_{caldera}$ $=1.10^{-15}$ m². Simulation runs have highlighted that a lower permeability tends to impact the groundwater loops and the mass flux orientation tend to evolved vertically within the shallower part. Then, it seems necessary to maintain a relatively high permeability in this unit to ensure the relevant groundwater loops described in the previous section and thermal anomalies surface observations (see conceptual model by Norini et al., (2015)). In order to assess the impact of the seal cap, a mesh refinement in this part of the model would be required.

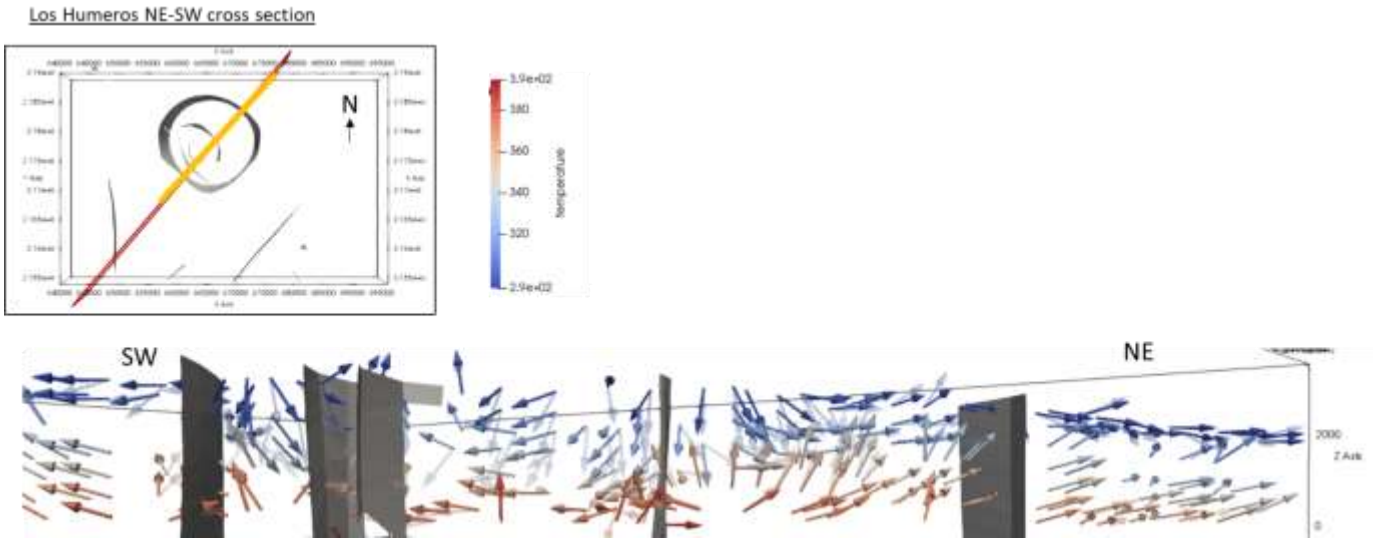

Figure 23: Influence of permeability variation in the Caldera formation on the simulated total mass flux orientation in the upper part of the model – screenshot of total mass flux, unscaled and colored with temperature (K) in the model over a NE-SW vertical cross section centered along LH and LP calderas with $K_{caldera}= 1.10^{-14}$ m² in (opaque colourful arrows) and $K_{caldera} = 1.10^{-15}$ m² (light transparent arrows)

Figure 24 shows the impact of the different permeability values for the basement formation. Two different permeabilities were considered for the matrix in the Basement: one of 1.10^{-15} m² and a lower one of 1.10^{-16} m² which is relatively higher than previously tested values (1.10^{-18} m²). Higher permeability for the basement facilitates convection processes and strongly impact the distribution of heat within the caldera. The permeability variation results in a change in location of the heat source up-flow position. Indeed for a permeability of 1.10^{-16} m², the up-flow is clearly localized at the centre of the caldera while when permeability in the Basement is defined at 1.10^{-15} m², the up-flow is localized in the south-western part of the caldera.

The permeability distribution within the model requires further investigation. A sensitivity analysis could be performed to assess the impact of the permeability of each unit on mass flux orientations and temperature in the shallower part to progress towards a better constrained model.

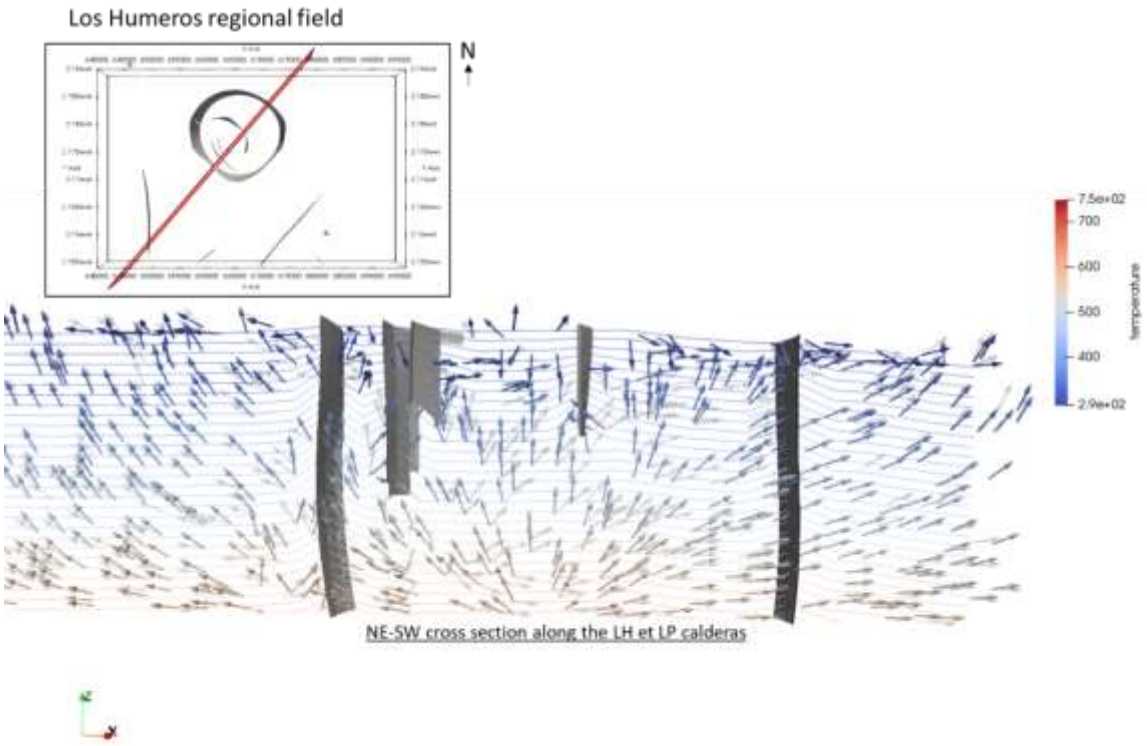

Figure 24: Influence of matrix permeability variation over temperature (K) and flow in the deeper part of the caldera – screenshot of total mass flux and temperature in the model over a NE-SW vertical cross section with $K_{matrix}=1.10^{-16}$ m² (opaque colourful arrows) and $K_{matrix}=1.10^{-15}$ m² (light transparent arrows).

4.3 Impact of the heat source location and power

The heat source, as presented in section 3.4, is assimilated to a magmatic chamber located below the caldera of LH and in the aplomb of LP caldera. The global heat flux in the model is 0.05 W/m² and an additional heat flux is set on facets of this estimated magmatic chamber, at the bottom of the model. Note that the additional flux decreases exponentially outside the cylinder.

The **influence of the additional heat flux**, reflecting the thermal structure present in LHVC, has been studied through sensitivity simulations at regional scale.

As observed on Figure 25, when only modifying the value of the heat flux inside the cylinder representing the magmatic heat source, the orientation of the flux is strongly impacted. Indeed, with larger flux, the heat is driven more directly towards the surface while a lower heat flux tends to generate a more radial conduction of heat. Hence, **strong flux are favoring transfer of heat through the faults.** The phenomenon is powerfully seen near the faults when looking at the temperature contours over the cross section in Figure 25, in the case of additional flux of 1 W/m² (bottom view).

These stronger fluxes directly influence the temperature profile within the caldera. An example is provided in Figure 26, where the strong flux highly increases temperature variations with depth, specifically where

geothermal wells are located. Nevertheless, this temperature profile is not consistent with the measured temperature located in this area (see Figure 8).

The results provided here demonstrate also a major influence of the temperature boundary imposed at the top. This boundary condition requires an improvement to progress towards a better understanding of the overall functioning of the hydrothermal system.

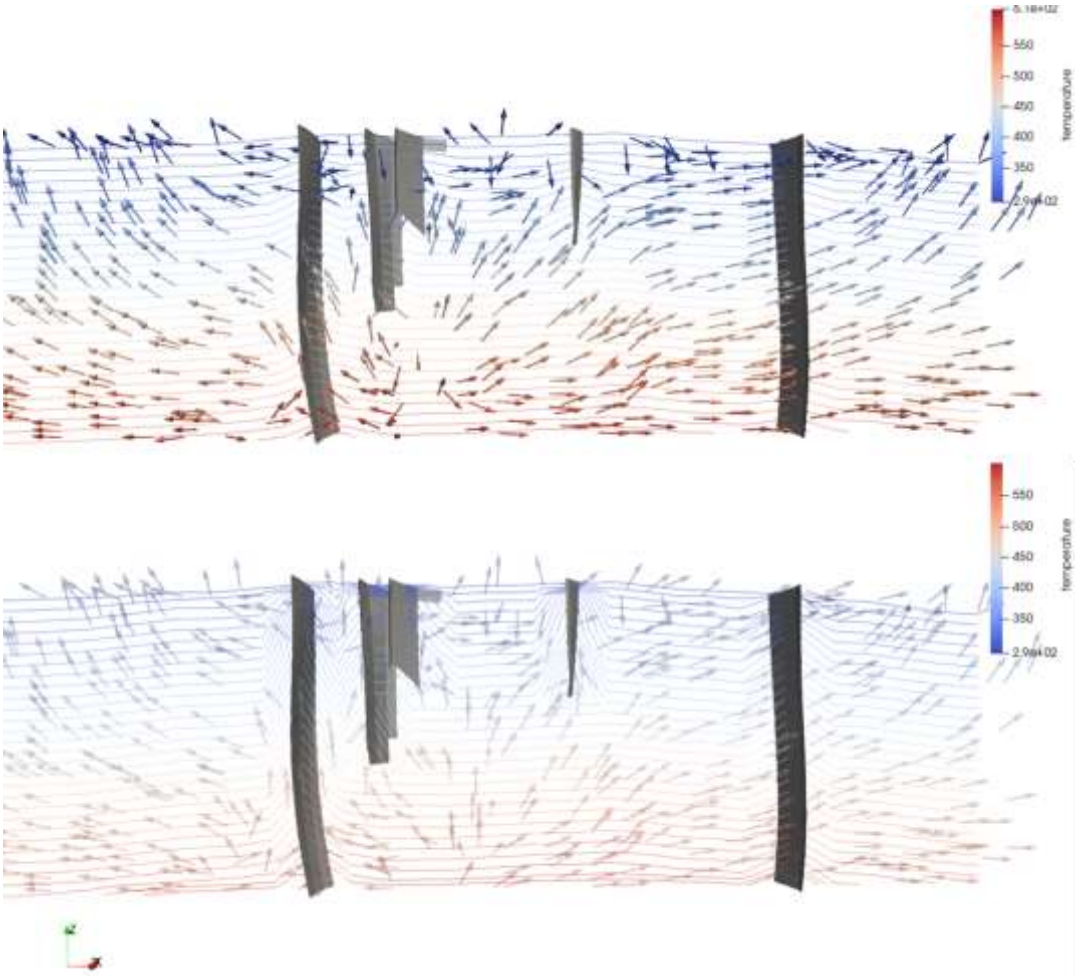

Figure 25: Comparison of temperature contour (in Kelvin) and mass flux orientation for heat source with additional heat flow 0.1 W/m² (top) and of 1 w/m² (bottom) along a NE-SW cross section intersecting LH and LP calderas

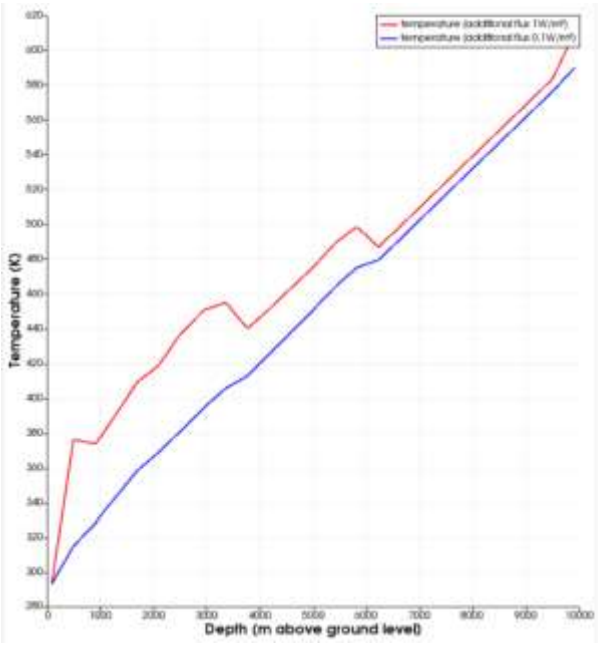

Location of temperature profile inside LP caldera

Figure 26: Left: Temperature as function of the depth inside LP caldera for additional heat source of 1 W/m² (red) or 0.1 W/m² (blue). Right: Location of the profile in the caldera

5 Improvement and development opportunities

5.1 Meshing

Meshing traditionally represents one of the main bottleneck when going from static models to dynamic models. The usual challenge is to achieve a trade-off between the overall mesh quality to be able to run correct (if not accurate) flow simulations with acceptable duration (typically no more than one night…) without an extreme degradation of the underlying geological geometries. This hurdle was still experiment for the work performed in the Gemex project and represent one the major difficulties encountered (cf. internship report by C. Barge (2018) for further details).

Considering that we want to promote an long term integration of the different modeling approaches (static vs. dynamic) we would like to be able to mesh the geological model seamlessly without modifying it because of flow simulation constraints (cf. section 3.2 with the model faults that were made vertical to produce a prismatic mesh). This is one of the major constraint to achieve an integrated model and possibly modify the geological model based on simulation outputs rather than input.

As the flow simulation tool used in this work (ComPASS) can handle correctly generic unstructured meshes we feel that the main axis of development is on the output of the geological modeling tool. Despite of the implementation of various unstructured meshing capabilities in the GeoModeller software, that were used for this project, we are still missing a flexible tool that can produce quality and hopefully anisotropic meshes out of 3D implicit geological models. One of the main short-term objective is to be able to extract a clean sealed *B-Rep* out of an implicit geological model as this will open the way to test other meshing algorithms (e.g. TetGen (Si, 2015) or new CGAL algorithms). This aspect will be studied in the forthcoming months.

Controls of the mesh refinement base on geological parameters were also lacking to be able to refine the mesh (and hence simulation results) in the main areas of interest. They are especially important to be able to perform convergence tests and achieve stable simulations. The refinement of the mesh will also help to differentiate

geological units and then simulate the impact of the seal cap at the top of the reservoir. Some preliminary tests can be performed with a prismatic extruded mesh with higher vertical resolution.

The initial geological model had no connection between the regional fault and the caldera. So modifying this would need to take into account the new geological model whose integration is planned for MS12 end of November 2019, the report is to be delivered in May 2020.

5.2 Permeability distribution and heat source position

Different positions of the heat source below the Los Humeros caldera have been tested during this work. Sensitivity analysis, varying the depth of the heat source below the caldera along with its vertical and/or radial extension did not permit to draw any conclusions concerning temperature distributions inside LHVC either at regional or local scale.

Further developments and new sensitivity tests with refined meshes should be perform to validate the hypothesis on the location of the heat source, the number of heat source (one magmatic chamber or various bodies), its power and how it heat transported towards the shallower formation of Los Humeros. It would also be worth investigating the development of convective zones around the intrusive magma (cf. the classical study by Hayba and Ingebritsen. (1997) where the area around the intrusion is considered to be more permeable and the latent heat of the magma is taken into account) and how this zones are connected to the main structures and generates an up-flow towards LHVC.

5.3 Boundary conditions at the top of the model

One of the major limitations in terms of model physics was the constant temperature and mass flux boundary conditions imposed on top of the model. Recently, Beaude *et al.* (in press) developed a new formulation for non-isothermal compositional gas Darcy flows and its coupling with an advanced soil-atmosphere boundary condition. The compositional model accounts for the water component, which can vaporize into the gas phase and for a set of gaseous components (typically air) which can dissolve into the liquid phase. The soil-atmosphere boundary condition, based on mole and energy balance equations set at the interface, takes into account the vaporization of the liquid phase in the atmosphere, the convective molar and energy transfer, a liquid outflow condition as well as the precipitation recharge and the heat radiation. This model is currently implemented into ComPASS and shall be available by mid-2019. It will allow for more realistic boundary condition model for the hydrothermal modeling of the Los Humeros area. Our goal is to rerun simulations with this new physics and gain more insight in the role of the main structural features (up-flow along faults and main location of outflows). We will then be able to observe the development of an unsaturated zone with a more realistic water table position and unbiased shallow ground temperature.

6 Conclusions

From a qualitative point of view, we achieved a distribution of flux and thermal anomalies at the regional scale of the Los Humeros Volcanic Complex which is consistent with the conceptual models proposed by Norini et al., (2015). Indeed, heat from deep basement formation is directed towards the north and south rim of Los Humeros caldera and over the south rim of Los Potreros caldera near the Antigua and Mastaloya faults.

However, to achieve a better integration between the 3D geological model of the area and its hydrothermal counterpart there are still bottlenecks concerning mainly mesh generation and the implementation of more realistic boundary conditions:

- the seamless generation of clean good quality meshes out of GeoModeller models needs improvement of the algorithm extracting an informed boundary representation of the geological models so that it can be used with various meshing algorithms – this work should be achieved on short term basis,
- the physical models available in ComPASS did not integrate atmospheric boundary conditions which would have been necessary to relax the hypothesis of an imposed shallow ground temperature on top of the model and let an unsaturated zone develop with a more realistic position of the water table – an advanced model for this boundary condition is currently implemented into ComPASS following the work of Beaude *et al.* (in press).

Finally, when a refined mesh is available, it might also be interesting to test the influence of permeability distributions on the shallow temperature profiles, where well data are available, and onto the partitioning into the top liquid dominated geothermal reservoir and the bottom vapour dominated geothermal reservoir.

7 Bibliography

Arellano, V.., García, A., Barragán, R.., Izquierdo, G., Aragón, A., Nieva, D., 2003. An updated conceptual model of the Los Humeros geothermal reservoir (Mexico). J. Volcanol. Geotherm. Res. 124, 67–88. https://doi.org/10.1016/S0377-0273(03)00045-3

Arellano, V.M., Barragán, R.M., Ramírez, M., et al., López, S., Paredes, A., Aragon, A., Tovar, R., 2015. The Response to Exploitation of the Los Humeros (México) Geothermal Reservoir, in: World Geothermal Congress 2015. Melbourne, Australia, p. 7.

Barge, C., 2018. Regional hydrothermal modeling of the Los Humeros system (Mexico).

Beaude, L., Brenner, K., Lopez, S., Masson, R., Smaï, F.F., n.d. Non-isothermal compositional liquid gas Darcy flow: formulation, soil-atmosphere boundary condition and application to high energy geothermal simulations. Comput. Geosci.

Brenner, K., Groza, M., Guichard, C., Lebeau, G., Masson, R., 2016. Gradient discretization of hybrid dimensional Darcy flows in fractured porous media. Numer. Math. 134, 569–609. https://doi.org/10.1007/s00211-015-0782-x

Brenner, K., Groza, M., Guichard, C., Masson, R., 2015. Vertex approximate gradient scheme for hybrid dimensional two-phase Darcy flows in fractured porous media. ESAIM Math. Model. Numer. Anal. 49, 303–330. https://doi.org/10.1051/m2an/2014034

Calcagno, P., Chilès, J.-P., Courrioux, G., Guillen, A., 2008. Geological modelling from field data and geological knowledge - Part I. Phys. Earth Planet. Inter. 171, 147–157. https://doi.org/10.1016/j.pepi.2008.06.013

Calcagno, P., Evanno, G., Trumpy, E., Gutiérrez-negrín, L.C., Luis, J., Vásquez, M., Carrasco, G., Liotta, D., 2019. 3D preliminary geological models of Los Humeros and Acoculco (Mexico) – H2020 GEMex project, in: Geophysical Research Abstracts EGU General Assembly 2018. p. 2020.

Calcagno, P., Evanno, G., Trumpy, E., Gutiérrez-Negrín, L.C., Macías, J.L., Carrasco-Núñez, G., Liotta, D., 2018. Preliminary 3-D geological models of Los Humeros and Acoculco geothermal fields (Mexico) – H2020 GEMex Project. Adv. Geosci. 45, 321–333. https://doi.org/10.5194/adgeo-45-321-2018

Campos-Enriquez, J., Garduño-Monroy, V.H., 1987. The shallow structure of Los Humeros and Las Derrumbadas geothermal fields, Mexico. Geothermics 16, 539–554. https://doi.org/10.1016/0375-6505(87)90038-1

Carrasco-Núñez, G., Bernal, J.P., Dávila, P., Jicha, B., Giordano, G., Hernández, J., 2018. Reappraisal of Los Humeros Volcanic Complex by New U/Th Zircon and 40 Ar/ 39 Ar Dating: Implications for Greater Geothermal Potential. Geochemistry, Geophys. Geosystems 19, 132–149. https://doi.org/10.1002/2017GC007044

Carrasco-Núñez, G., López-Martínez, M., Hernández, J., Vargas, V., 2017. Subsurface stratigraphy and its correlation with the surficial geology at Los Humeros geothermal field, eastern Trans-Mexican Volcanic Belt. Geothermics 67, 1–17. https://doi.org/10.1016/j.geothermics.2017.01.001

Caumon, G., Lepage, F., Sword, C.H., Mallet, J.-L., 2004. Building and Editing a Sealed Geological Model. Math. Geol. 36, 405–424. https://doi.org/10.1023/B:MATG.0000029297.18098.8a

Cedillo Rodríguez, F., 2000. Hydrogeologic Model of the Geothermal Reservoirs From Los Humeros, Puebla, Mexico, in: World Geothermal Congress 2000. Kyushu - Tohoku, Japan, pp. 1639–1644.

Cedillo Rodríguez, F., 1999. Modelo hidrogeológico de los yacimientos geotérmicos de Los Humeros, Pue., México., Geotermia, Rev. Mex. de Geoenergía.

Coats, K.H.H., 1989. Implicit Compositional Simulation of Single-Porosity and Dual-Porosity Reservoirs. SPE Symp. Reserv. Simul. https://doi.org/10.2118/18427-MS

Droniou, J., Eymard, R., Herbin, R., 2016. Gradient schemes: Generic tools for the numerical analysis of diffusion equations. ESAIM Math. Model. Numer. Anal. 50, 749–781. https://doi.org/10.1051/m2an/2015079

Eymard, R., Guichard, C., Herbin, R., Masson, R., 2012. Vertex-centred discretization of multiphase compositional Darcy flows on general meshes. Comput. Geosci. 16, 987–1005. https://doi.org/10.1007/s10596-012-9299-x

Ferrari, L., López-martínez, M., Aguirre-díaz, G.J., Carrasco-núñez, G., Ferrari, L., Geología, I. De, Nacional, U., México, A. De, Postal, A., Universitaria, C., Aguirre-díaz, G., Carrasco-núñez, G., Postal, A., California, B., 1999. Space-time patterns of Cenozoic arc volcanism in central Mexico : From the Sierra Madre Occidental to the Mexican Volcanic Belt Space-time patterns of Cenozoic arc volcanism in central Mexico : From the Sierra Madre Occidental to the Mexican Volcanic Belt. Geology 27, 303–306.

Goutorbe, B., Lucazeau, F., Bonneville, A., 2007. Comparison of several BHT correction methods: a case study on an Australian data set. Geophys. J. Int. 170, 913–922. https://doi.org/10.1111/j.1365-246X.2007.03403.x

Gutiérrez-Negrín, L.C., Montalvo, G.I., Aguilar, A.A., 2010. Review and Update of the Main Features of the Los Humeros Geothermal Field, Mexico. Geotherm. Resour. Counc. Trans. 34, 765–770.

Hayba, D.O., Ingebritsen, S.E., 1997. Multiphase groundwater flow near cooling plutons. J. Geophys. Res. 102, 12235–12252.

IEA Geothermal, 2018. 2017 Annual Report. https://doi.org/10.3987/Contents-06-70

Jentsch, A., Jolie, E., 2017. Systematic soil gas studies for volcano-tectonic analyses of the Los Humeros Geothermal Field, Mexico, in: Cities on Volcanoes 10. Napoli (Italy).

Jimenez-Salgado, E., 2014. Estudio Geohidrologico en el campo geotermico de Los Humeros, PUE.

Lajaunie, C., Courrioux, G., Manuel, L., 1997. Foliation Fields and 3D Cartography in Geology : Principles of a Method Based on Potential Interpolation. Math. Geol. 29, 571–584.

Limberger, J., Bonté, D., van Wees, J.-D., 2018. Thermal structure of Los Humeros: Estimating magma chamber emplacement depth by inverse modelling of temperature measurements.

López-Hernández, A., 1995. Estudio regional volcanico y estructural del campo geotermico de Los humeros. Rev. Mex. Geonergia 11, 17–36.

Lopez, S., Masson, R., Beaude, L., Birgle, N., Brenner, K., Kern, M., Smaï, F., Xing, F., 2018. Geothermal Modeling in Complex Geological Systems with the ComPASS Code, in: 43rd Workshop on Geothermal Reservoir Engineering. Stanford, United States.

Norini, G., Groppelli, G., Sulpizio, R., Carrasco-Núñez, G., Dávila-Harris, P., Pellicioli, C., Zucca, F., De Franco, R., 2015. Structural analysis and thermal remote sensing of the Los Humeros Volcanic Complex: Implications for volcano structure and geothermal exploration. J. Volcanol. Geotherm. Res. 301, 221–237. https://doi.org/10.1016/j.jvolgeores.2015.05.014

Pruess, K., 1992. Brief Guide to the MINC-Method for Modeling Flow and Transport in Fractured Media. Lawrence Berkeley Laboratory, University of California.

Rineau, L., Yvinec, M., 2007. A generic software design for Delaunay refinement meshing. Comput. Geom. 38, 100–110. https://doi.org/10.1016/j.comgeo.2006.11.008

Si, H., 2015. TetGen, a Delaunay-Based Quality Tetrahedral Mesh Generator. ACM Trans. Math. Softw. 41, 1–36. https://doi.org/10.1145/2629697

Torres-Rodriguez, M.A., 1993. Características del Yacimiento contenido en el campo de Los Los Humeros, Puebla, Ingenieria de yacimientos, Informe OIY-HU- 10/93 C.F.E.

Tovar, R., López, O., 1998. Comportamiento Geoquímico e isotópico del fluido de los pozos del campo geotérmico Los Humeros, Puebla, México, in: Meeting Los Azufres Mich. OIEA-CFE.

Viggiano, J.C., C., R., 1988. Mineralogía Hidrotermal en el campo geotérmico Los Humeros, Puebla, Tomo I: Sus usos como Inducadora de temperatura del régimen Hidrológico. Hidrológico, Geoterm. 4.

Xing, F., Masson, R., Lopez, S., 2017. Parallel numerical modeling of hybrid-dimensional compositional non-isothermal Darcy flows in fractured porous media. J. Comput. Phys. 345, 637–664. https://doi.org/10.1016/j.jcp.2017.05.043

Coordination Office, GEMex project

Helmholtz-Zentrum Potsdam
Deutsches GeoForschungsZentrum

Telegrafenberg, 14473 Potsdam

Germany